



NRL/MR/5653--99-8419

# **An Introduction to ARRSTATS — A Computer Program for Simulating the Effects of Errors in Time- and Phase- Steered Planar Array Antennas**

C. STAN WEST

*Photonics Technology Branch  
Optical Sciences Division*

November 22, 1999

Approved for public release; distribution unlimited.

20000104 049

REPORT DOCUMENTATION PAGE			Form Approved OMB No. 0704-0188	
Public reporting burden for this collection of information is estimated to average 1 hour per response, including the time for reviewing instructions, searching existing data sources, gathering and maintaining the data needed, and completing and reviewing the collection of information. Send comments regarding this burden estimate or any other aspect of this collection of information, including suggestions for reducing this burden, to Washington Headquarters Services, Directorate for Information Operations and Reports, 1215 Jefferson Davis Highway, Suite 1204, Arlington, VA 22202-4302, and to the Office of Management and Budget, Paperwork Reduction Project (0704-0188), Washington, DC 20503.				
1. AGENCY USE ONLY (Leave Blank)	2. REPORT DATE  November 22, 1999	3. REPORT TYPE AND DATES COVERED  Final		
4. TITLE AND SUBTITLE  An Introduction to ARRSTATS — A Computer Program for Simulating the Effects of Errors in Time- and Phase-Steered Planar Array Antennas		5. FUNDING NUMBERS  ONR — 63217N		
6. AUTHOR(S)  C. Stan West				
7. PERFORMING ORGANIZATION NAME(S) AND ADDRESS(ES)  Naval Research Laboratory Washington, DC 20375-5320		8. PERFORMING ORGANIZATION REPORT NUMBER  NRL/MR/5653--99-8419		
9. SPONSORING/MONITORING AGENCY NAME(S) AND ADDRESS(ES)  Bobby Junker Office of Naval Research		10. SPONSORING/MONITORING AGENCY REPORT NUMBER		
11. SUPPLEMENTARY NOTES				
12a. DISTRIBUTION/AVAILABILITY STATEMENT  Approved for public release; distribution unlimited.			12b. DISTRIBUTION CODE	
13. ABSTRACT (Maximum 200 words)  A computer program is described that simulates time- and phase-steered array antennas subject to deterministic and random errors. The modeled array comprises a planar, rectangular grid of phase-steered elements grouped hierarchically into time-steered subarrays and time-steered subapertures. Random phase, time, and amplitude errors may be assigned, and the phases and times may be quantized. The simulation frequency may differ from the design frequency. The program assesses the antenna's performance by computing and analyzing the far-field radiation pattern or an ensemble of statistically identical patterns. It determines the location and power density of the main beam peak, the pointing error, the major and minor beam widths, the directivity, the ratio of main beam and sidelobe powers, and other measures. The program can tabulate measures as functions of a user-specified independent variable such as the operating frequency, a steering angle, an error parameter, a quantization specification, or a parameter of the array geometry. Results may be displayed as textual output of the performance measures, plots of radiation patterns, and plots of performance measures versus the independent variable.				
14. SUBJECT TERMS			15. NUMBER OF PAGES  54	
			16. PRICE CODE	
17. SECURITY CLASSIFICATION OF REPORT  UNCLASSIFIED	18. SECURITY CLASSIFICATION OF THIS PAGE  UNCLASSIFIED	19. SECURITY CLASSIFICATION OF ABSTRACT  UNCLASSIFIED	20. LIMITATION OF ABSTRACT  UL	

## CONTENTS

1. INTRODUCTION .....	1
2. COORDINATE SYSTEMS AND PROJECTIONS .....	2
3. ARRAY PARAMETERS .....	4
4. EXCITATIONS .....	6
4.1. Error-Free Excitations .....	6
4.2. Erroneous Excitations .....	8
5. RADIATION PATTERN .....	9
6. PATTERN MEASURES .....	9
6.1. Pointing Vector, Pointing Error, and Peak Power Density .....	10
6.2. Main Beam Region .....	11
6.3. Main Beam Width and Roll .....	11
6.4. Directivity, Power Ratios, and Average Sidelobe Level .....	12
6.5. Powers and Distances of Largest and Nearest Sidelobes .....	13
7. MULTIPLE REALIZATIONS AND PARAMETER VALUES .....	13
8. PROGRAM OUTPUT .....	13
9. SUMMARY .....	15
APPENDIX A — LIST OF VARIABLES .....	17
APPENDIX B — PROGRAM LISTING .....	19
REFERENCES .....	49

# AN INTRODUCTION TO ARRSTATS — A COMPUTER PROGRAM FOR SIMULATING THE EFFECTS OF ERRORS IN TIME- AND PHASE-STEERED PLANAR ARRAY ANTENNAS

## 1. INTRODUCTION

Phased array antennas are remarkable for their suitability to many applications, which is partly because they steer quickly, allow adaptive processing, conform to special shapes, and produce a variety of radiation patterns. As low-sidelobe radiation patterns were being developed, it became apparent that errors in the phase or amplitude of the element excitations would limit the lowest achievable sidelobe level. Such errors might be due to manufacturing tolerances on the physical structure, inaccurate phase shifters, or non-uniform feeds, and can affect the average and peak sidelobe levels, beam width, pointing accuracy, and directivity, for example. Although one cannot predict the performance of a given antenna without measurements of the phase and amplitude accuracy of each element, one can draw conclusions about the behavior of an ensemble of antennas that are statistically identical but have different realizations of phase and amplitude errors. The present work applies this approach to a generalized array antenna that blends phase- and time-steering to achieve greater bandwidth at a reasonable cost.<sup>1-3</sup> The purpose of this report is to introduce the reader to a computer program for simulating time- and phase-steered planar array antennas subject to deterministic and random excitation errors. It is intended as an overview to the features and capabilities of the program and a guide to understanding the program's input, processing, and output.

The theoretical study of errors in array antennas has produced a large body of literature. Introductions to these works and key results and derivations may be found in several books.<sup>4-6</sup> The literature on simulations is more sparse, but two programs have been described recently against which this work may be contrasted. First, Chrisman<sup>7</sup> describes a program that simulates phase-steered planar arrays. It computes the directivity and cuts of the design and expected radiation patterns from the error statistics using theoretical formulas. One pattern cut intersects the main beam and boresight, and the other is normal to it through the main beam; from them the beam width is obtained in those directions. Second, Wright<sup>8</sup> briefly discusses the features of a simulation of phase-steered arrays. Its parameters include phase and amplitude errors, number of quantization bits, and bandwidth, and it can output two-dimensional beam patterns, sidelobe statistics, and measures of specialized interest. The program discussed here, called ARRSTATS, differs from those in Refs. 7 and 8 primarily in that it can model arrays with a hybrid phase- and time-steered architecture,<sup>9</sup> including strictly phased arrays and strictly time-steered arrays.<sup>10</sup> Also, it computes individual realizations of the hemispherical radiation pattern and obtains most measures of the array performance directly from the full pattern rather than from formulas or from pattern cuts chosen *a priori*. (Ref. 8 does not specify how its performance measures are obtained.) For example, the beam width cuts are always along the major and minor axes of the beam width ellipse, regardless of its orientation. Another special feature is a method for locating the beam peak that is highly accurate for nearly flat phase fronts; it is the only measure not obtained directly from the radiation pattern.

In more detail, the modeled array comprises a rectangular grid of phase-steered elements; these

are grouped into time-steered subarrays, which in turn are grouped into time-steered subapertures. The phases and times may be quantized. A random phase error may be associated with the elements, and random time errors may be assigned to the subarrays and subapertures. Also, random amplitude errors may be associated with the elements, subarrays, and subapertures. The user specifies the design frequency, at which the error-free times and phases would correctly steer the antenna, and the operating frequency, at which the array's behavior is simulated. The antenna may be steered to any direction. ARRSTATS assesses the array's performance by computing and analyzing the far-field radiation pattern or an ensemble of statistically identical patterns. It ignores polarization and mutual coupling between elements and assumes that the elements radiate uniformly into the forward hemisphere. For each computed pattern, it determines the following:

- the location and power density of the main beam peak
- the error in the main beam's location
- the main beam's angular limits, major and minor widths at half power, and orientation
- the directivity
- the ratios of powers in the main beam, sidelobes, and the radiation hemisphere
- the powers and distances of the sidelobes that are strongest and nearest to the main beam

Furthermore, it can track these measures as functions of a user-specified independent variable. ARRSTATS provides textual output of the performance measures, plots of radiation patterns, and plots of performance measures versus the independent variable.

ARRSTATS is a script written for version 5.3 of MATLAB, a commercial software package for technical computing.<sup>11</sup> Some elements of the program structure and some of the graphics facilities take advantage of features in version 5.3, but much of the code is compatible with earlier versions of MATLAB. ARRSTATS consists of one text file and is executed by typing its filename at the MATLAB command prompt. The program does not have an input user interface; instead, the user hardcodes input into the script before execution. These input points are tagged with the word "INPUT" in the code's comments.

The remainder of this report is structured as follows. Section 2 introduces the coordinate systems used for input and output, Section 3 explains the input parameters that describe the array, Section 4 specifies the model for the excitations, and Section 5 outlines the calculation of the radiation pattern. Section 6 describes the pattern measures, Section 7 discusses looping over multiple realizations and parameter values, and Section 8 exhibits the program's output. Two appendices are provided: Appendix A relates the variables used in this report and in the program, and Appendix B is a listing of the program code. Most of the report aims to describe aspects of the program's operation but does not give the details of the implementation or algorithms. The interested reader is directed to the code listing, specifically the comments that introduce each section of the program. Throughout this report, code variables are printed in a monospaced face, and braces ({} ) enclose references to code line numbers except where the context suggests set notation.

## 2. COORDINATE SYSTEMS AND PROJECTIONS

ARRSTATS internally uses a three-dimensional Cartesian coordinate system to describe space. The array lies in the  $x$ - $y$  plane and radiates into the half-space  $z > 0$ , as in Figure 1. (Although we describe a transmitter array, the case for a receiver array is identical.) The far-field spatial distribution of this radiation — that is, the radiation pattern — is a function of direction in the half-space. Two variables suffice to specify direction, and several pairs of variables are useful for this purpose. First, direction

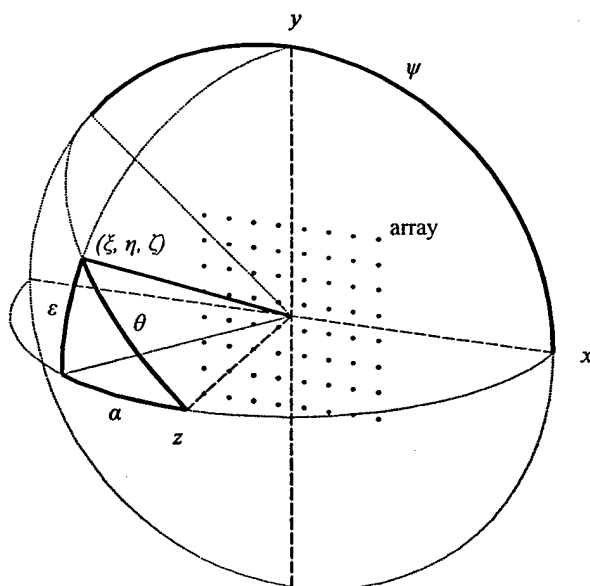


Figure 1 — Cartesian and spherical coordinates;  $\theta$ ,  $\psi$ ,  $\alpha$ , and  $\varepsilon$  are shown positive

cosines are the natural coordinates for calculating the array factor, as will be seen later. The direction cosines for a given direction are simply the Cartesian coordinates  $(\xi, \eta, \zeta)$  of the corresponding unit vector. Specifying a direction in the half-space  $z > 0$  requires only  $\xi$  and  $\eta$ ;  $\zeta$  may be obtained from the unit vector constraint if needed. Second, spherical coordinates are convenient for constructing flat projections of the radiation pattern, as it may be regarded as a function of location on a (curved) hemisphere. As shown in Figure 1, the polar angle  $\theta$  for a given vector is the angle between the positive  $z$  axis and the vector, while the azimuth angle  $\psi$  is the angle between the positive  $x$  axis and the projection of the vector onto the  $x$ - $y$  plane. Third, traditional antenna coordinates connect these simulations to an established context. Given the projection of a vector onto the  $x$ - $z$  plane, the azimuth angle  $\alpha$  is the angle between the projection and the  $z$  axis, while the elevation angle  $\varepsilon$  is the angle between the projection and the vector. These three sets of coordinates are related according to

$$\begin{aligned}\xi &= \sin \theta \cos \psi = -\cos \varepsilon \sin \alpha \\ \eta &= \sin \theta \sin \psi = \sin \varepsilon \\ \zeta &= \cos \theta = \cos \varepsilon \cos \alpha\end{aligned}\tag{1}$$

$$\begin{aligned}\cos \theta &= \cos \varepsilon \cos \alpha = \zeta \\ \tan \psi &= -\tan \varepsilon / \sin \alpha = \eta / \xi\end{aligned}\tag{2}$$

$$\begin{aligned}-\tan \alpha &= \xi / \zeta = \tan \theta \cos \psi \\ \sin \varepsilon &= \eta = \sin \theta \sin \psi.\end{aligned}\tag{3}$$

ARRSTATS also employs three projections of the hemisphere onto flat two-dimensional space: orthographic, Lambert azimuthal, and stereographic. The orthographic projection yields a view of the hemisphere from a particular vantage point without perspective distortion and is available for displaying the radiation pattern. The remaining projections both map the hemisphere to a disk such that boresight

corresponds to the center of the disk and grazing directions correspond to the perimeter of the disk. To describe these projections more specifically, we denote locations on the disk using polar coordinates (radius and angle). For both projections, the angular coordinate is set equal to the spherical azimuth angle  $\psi$ ; the mapping from the spherical polar angle  $\theta$  to the radius  $r$  distinguishes the two projections.

The Lambert projection preserves relative area: the ratio of two areas on the hemisphere equals that of the corresponding areas on the projected disk.<sup>12</sup> This property may be expressed by equating (to a proportionality constant) the spherical and planar surface areas:

$$\sin \theta d\theta d\psi = C r_L dr_L d\psi, \quad (4)$$

where the subscript "L" distinguishes the radius in the Lambert projection from that in the stereographic projection below. Canceling  $d\psi$  and integrating both sides produces an integration constant, whose value and that of  $C$  are determined by the constraints that  $r_L = 0$  when  $\theta = 0$  and  $r_L = 1$  when  $\theta = \pi/2$ . One finds

$$r_L = \sqrt{2} \sin \frac{\theta}{2}, \quad (5)$$

which deviates only slightly from a linear relationship for  $\theta \in [0, \pi/2]$ . When the radiation pattern is plotted with the Lambert projection, the areas occupied by structures such as the main beam and sidelobes are in true proportion to each other and to the total area.

While the stereographic projection does not preserve area, it is conformal.<sup>12</sup> The local scale is uniform in any direction; shape is preserved locally. Great and small circles on the hemisphere are projected into circles or straight lines, and the angle between two great circles on the hemisphere equals the angle at the intersection of their projected images. To derive the governing relationship, equate the aspect ratios of orthogonal derivatives, as

$$\frac{d\theta}{\sin \theta d\psi} = \frac{dr_s}{r_s d\psi}, \quad (6)$$

where the subscript "S" denotes the stereographic projection. Canceling and integrating as before yields

$$r_s = \tan \frac{\theta}{2}. \quad (7)$$

ARRSTATS internally uses the stereographic projection when identifying the major and minor axes of the beamwidth ellipse (see Section 6.3) and makes it available for plotting the radiation pattern.

### 3. ARRAY PARAMETERS

Several parameters describe the antenna's geometry and associated frequencies {29–94}. As Figure 2 illustrates, the antenna elements occupy a regular rectangular grid in the  $x$ - $y$  plane; the element spacings in each dimension,  $d_x$  and  $d_y$ , may differ. The elements are grouped hierarchically at three levels. The array is subdivided into  $L_x$  by  $L_y$  subapertures, each of which has an associated time delay for steering. Descending to the next level, each subaperture contains  $M_x$  by  $M_y$  subarrays, each of which likewise has a steering time delay. Finally, each subarray contains  $N_x$  by  $N_y$  elements, each of which is phase-steered. Regular element spacing is maintained across subarray and subaperture boundaries. To

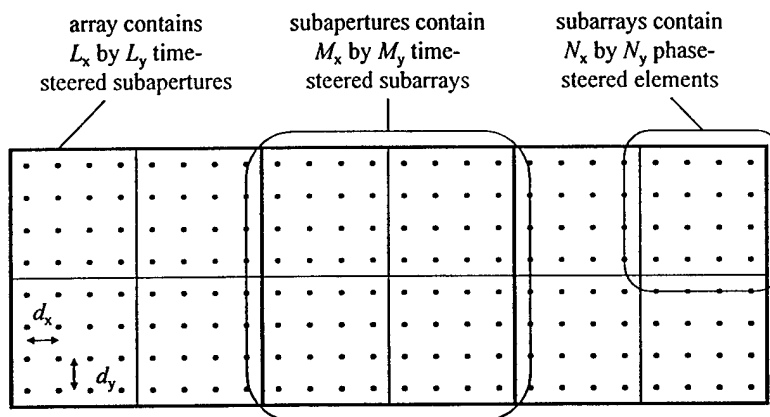


Figure 2 — Array structure and geometry

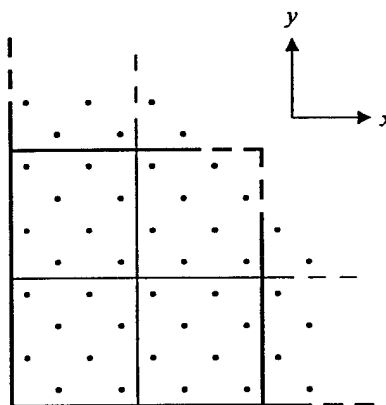


Figure 3 — Element layout when diamond flag is nonzero

simulate an array with one time-steered level and one phase-steered level,  $L_x$  and  $L_y$  should be set to 1; for a strictly phased array, also set  $M_x$  and  $M_y$  to 1. On the other hand, one may model a strictly time-steered array with one or two hierarchical levels by setting  $N_x$  and  $N_y$  to 1 and  $\delta\phi$  to  $360^\circ$  (this renders the phase shifters ineffective; see Section 4.1).

Two additional program parameters specify special antenna geometries. If the flag `diamond` is nonzero, elements are effectively removed from even diagonals (the zeroth diagonal originates at the lower-left element), leaving a diamond pattern of active elements as in Figure 3. The parameter `azmthOffst` rotates the antenna about the  $z$  axis (boresight); it is the angle of the positive  $x$  axis of the array above the azimuth reference. Within ARRSTATS, all calculations are performed in the antenna coordinate system; the steering vector provided by the user is transformed to the antenna coordinate system before processing, and output coordinates and plotted structures are transformed from the antenna coordinate system after processing.



Finally, two parameters supply frequency information. The reference or design frequency  $f_0$  is that at which the time and phase delays would correctly steer the antenna in the absence of error and quantization. The operating frequency  $f$  is that at which the simulation is to be performed. Multiple frequencies may be considered sequentially as described in Section 7.

#### 4. EXCITATIONS

##### 4.1. Error-Free Excitations

We now construct the element excitations in detail to show the structure of the array model, beginning with the error-free case {338–410}. Because only one frequency is considered at a time, time delays may be expressed as equivalent phase delays. We therefore decompose the excitations into magnitude and phase as

$$\bar{a}_{n_x n_y} = |\bar{a}_{n_x n_y}| \exp(-i\bar{\Phi}_{n_x n_y}), \quad n_w \in \{0, 1, \dots, L_w M_w N_w - 1\}, \quad w \in \{x, y\}, \quad (8)$$

where the overbars indicate the error-free case and the  $n_w$  label the elements across the face of the array, ignoring subaperture and subarray boundaries. The error-free magnitudes are made equal for all active elements and normalized to unit total power, so that

$$\sum_{n_x} \sum_{n_y} |\bar{a}_{n_x n_y}|^2 = 1. \quad (9)$$

The phases are derived from the condition that at the reference frequency the far-field radiation must interfere perfectly constructively in the direction of the steering vector. This implies that the phase must progress linearly across the face of the array as

$$\bar{\Phi}_{n_x n_y} = -k_0(d_x s_x n_x + d_y s_y n_y) + \text{const.}, \quad (10)$$

where  $k_0 = 2\pi f_0 / c$  is the reference wave number and  $(s_x, s_y)$  are the direction cosines of the steering vector {96–166}. Considering the architecture of the array, the phases must be built up from the equivalent time delays at the subaperture and subarray levels and the phase delays at the element levels. Based on Eq. (10), the phase step in direction  $w$  between adjacent elements in a subarray must be

$$\Delta\phi_w = -k_0 d_w s_w. \quad (11)$$

Likewise, since each subarray contains  $N_x$  by  $N_y$  elements, adjacent subarrays within a subaperture must have a phase difference of  $N_w \Delta\phi_w$ , which is equivalent to a time step

$$\begin{aligned} \Delta t_w &= \frac{1}{\omega_0} N_w \Delta\phi_w \\ &= -\frac{1}{c} N_w d_w s_w, \end{aligned} \quad (12)$$

where  $\omega_0 = 2\pi f_0$  is the reference angular frequency, and the time step across subapertures follows similarly as

$$\Delta T_w = -\frac{1}{c} N_w M_w d_w s_w. \quad (13)$$

In practical arrays, the time and phase delays are often quantized, leading to violations of Eq. (10) for general steering angles. We suppose that the beamformer is capable of mitigating the effects of subaperture and subarray quantization by adjusting the subarray and element delays. That is, the delay lost or gained in each subaperture due to quantization can be balanced by additional or reduced delay in the subarrays, assuming that the quantization interval of the subarrays is less than that of the subapertures. Likewise, the error due to subarray quantization can be balanced by adjusting the element phases, subject to a similar assumption. To exhibit this scheme mathematically, we introduce the subaperture, subarray, and element quantization intervals  $\delta T$ ,  $\delta t$ , and  $\delta\phi$ , respectively. We also introduce subaperture labels  $l_x$  and  $l_y$  and subarray labels  $m_x$  and  $m_y$ ; as the  $n_w$  ignore subaperture and subarray boundaries, so the  $m_w$  ignore subarray boundaries. More specifically, we obtain the  $l_w$  and  $m_w$  from the  $n_w$  according to

$$\begin{aligned} l_w &= \left\lfloor \frac{n_w}{N_w M_w} \right\rfloor, \quad l_w \in \{0, 1, \dots, L_w - 1\}, \quad \text{and} \\ m_w &= \left\lfloor \frac{n_w}{N_w} \right\rfloor, \quad m_w \in \{0, 1, \dots, L_w M_w - 1\}, \end{aligned} \quad (14)$$

where  $\lfloor x \rfloor$  is the greatest integer not exceeding  $x$ .

We define the subaperture time delays without quantization or error to be

$$\bar{T}_{n_x n_y} = l_x \Delta T_x + l_y \Delta T_y, \quad (15)$$

where the  $l_w$  are implicitly dependent upon the  $n_w$ , and the quantized subaperture time delays are then

$$\hat{T}_{n_x n_y} = \delta T \text{round}(\bar{T}_{n_x n_y} / \delta T), \quad (16)$$

where  $\text{round}(x)$  is the integer nearest  $x$ . The subarray time delays contain an additional term that compensates for the subaperture quantization:

$$\begin{aligned} \bar{t}_{n_x n_y} &= m_x \Delta t_x + m_y \Delta t_y - \hat{T}_{n_x n_y}, \\ \hat{t}_{n_x n_y} &= \delta t \text{round}(\bar{t}_{n_x n_y} / \delta t), \end{aligned} \quad (17)$$

where the  $m_w$  are implicitly dependent upon the  $n_w$ , and the element phase delays contain two similar terms:

$$\begin{aligned} \bar{\phi}_{n_x n_y} &= n_x \Delta \phi_x + n_y \Delta \phi_y - \omega_0 (\hat{T}_{n_x n_y} + \hat{t}_{n_x n_y}), \\ \hat{\phi}_{n_x n_y} &= \delta \phi \text{round}(\bar{\phi}_{n_x n_y} / \delta \phi) \end{aligned} \quad (18)$$

In so defining the delays, we have implicitly chosen the constant in Eq. (10) to be zero. This choice implies that the lowest and leftmost components (those with  $l_w = 0$ ,  $m_w = 0$ , or  $n_w = 0$ ) have no associated delay regardless of the steering vector, whereas the highest and rightmost components (having  $l_w =$

$L_w - 1$ ,  $m_w \bmod M_w = M_w - 1$ , or  $n_w \bmod N_w = N_w - 1$ ) have delays that depend strongly on the steering vector.

In the program, quantization may be avoided by setting the quantization steps to zero. The above equations are then equivalent to

$$\begin{aligned}\bar{T}_{n_x n_y} &= \hat{T}_{n_x n_y} = l_x \Delta T_x + l_y \Delta T_y, \\ \bar{t}_{n_x n_y} &= \hat{t}_{n_x n_y} = (m_x \bmod M_x) \Delta t_x + (m_y \bmod M_y) \Delta t_y, \quad \text{and} \\ \bar{\varphi}_{n_x n_y} &= \hat{\varphi}_{n_x n_y} = (n_x \bmod N_x) \Delta \phi_x + (n_y \bmod N_y) \Delta \phi_y.\end{aligned}\tag{19}$$

We note that  $m_w \bmod M_w$  is the index of subarray  $m_w$  within its parent subaperture, and likewise  $n_w \bmod N_w$  is the index of element  $n_w$  within its parent subarray.

For each element, the net (possibly quantized) phase at the operating frequency is the sum of equivalent phase contributions from the three hierarchical levels:

$$\hat{\Phi}_{n_x n_y} = \omega(\hat{T}_{n_x n_y} + \hat{t}_{n_x n_y}) + \hat{\varphi}_{n_x n_y},\tag{20}$$

where  $\omega = 2\pi f$  is the operating angular frequency. This quantized phase assumes the place of  $\Phi_{n_x n_y}$  in Eq. (8). At the reference frequency ( $\omega = \omega_0$ ) and with no phase quantization, this construction of the phase yields the linear progression of Eq. (10).

#### 4.2. Erroneous Excitations

We model the errors in a real antenna by applying amplitude and phase errors to each level of the antenna hierarchy {525-549}. Amplitude errors multiply the error-free amplitudes by factors of the form  $1 + \rho$  where  $\rho$  is a random number, distributed normally with zero mean. Each level contributes such errors, so that the erroneous amplitude for element  $(n_x, n_y)$  is

$$|a_{n_x n_y}| = |\bar{a}_{n_x n_y}| (1 + R_{l_x l_y}) (1 + r_{m_x m_y}) (1 + \rho_{n_x n_y}),\tag{21}$$

where  $R$ ,  $r$ , and  $\rho$  correspond to subapertures, subarrays, and elements, respectively. This model allows corresponding elements in different subarrays to contribute distinct errors, and likewise for corresponding subarrays within different subapertures. The user specifies the standard deviations  $\sigma_R$ ,  $\sigma_r$ , and  $\sigma_\rho$  of the respective amplitude errors.

Time and phase errors add to the error-free (but possibly quantized) time and phase delays. The subapertures and subarrays contribute random time errors  $\tilde{T}$  and  $\tilde{t}$ , respectively, and the elements contribute random phase errors  $\tilde{\varphi}$ , all drawn from zero-mean normal distributions. The user specifies the corresponding standard deviations  $\sigma_T$ ,  $\sigma_t$ , and  $\sigma_\varphi$ . Additionally, the user may specify a deterministic time error  $\mathcal{F}$  for each subaperture. The net equivalent phase error for element  $(n_x, n_y)$  is

$$\tilde{\Phi}_{n_x n_y} = \omega(\mathcal{F}_{l_x l_y} + \tilde{T}_{l_x l_y} + \tilde{t}_{m_x m_y}) + \tilde{\varphi}_{n_x n_y},\tag{22}$$

and the total erroneous phase is the sum of the quantized and error phases:

$$\Phi_{n_x n_y} = \hat{\Phi}_{n_x n_y} + \tilde{\Phi}_{n_x n_y}. \quad (23)$$

Finally, the erroneous complex excitations are

$$a_{n_x n_y} = |a_{n_x n_y}| \exp(-i\Phi_{n_x n_y}). \quad (24)$$

## 5. RADIATION PATTERN

In standard array theory with mutual coupling ignored, the field pattern is the product of the array factor and the element factor. In ARRSTATS, the element factor is unity, corresponding to uniform hemispherical radiation, so the field pattern equals the array factor. (See the code {2595–2715} for notes on expanding ARRSTATS.) Given the complex excitations, the array factor (and field pattern) in the direction  $(\xi, \eta)$  is given by the two-dimensional Fourier transform {551–561}

$$g(\xi, \eta) = \sum_{n_x} \sum_{n_y} \exp[-ik(\xi d_x n_x + \eta d_y n_y)] a_{n_x n_y}, \quad (25)$$

where  $k = 2\pi f / c$  is the operating wave number. ARRSTATS uses a fast Fourier transform to obtain  $g$  in discrete directions given by

$$\begin{aligned} \xi_{q_x} &= \frac{2\pi q_x}{k d_x Q_x}, \quad q_x \in \{0, 1, \dots, Q_x - 1\}, \quad \text{and} \\ \eta_{q_y} &= \frac{2\pi q_y}{k d_y Q_y}, \quad q_y \in \{0, 1, \dots, Q_y - 1\}, \end{aligned} \quad (26)$$

where  $Q_x$  and  $Q_y$  are the number of points in the transform in each dimension {168–173}. The  $(\xi_{q_x}, \eta_{q_y})$  grid is extrapolated to all of visible space using {412–497, 558}

$$\begin{aligned} g(\xi_{q_x + Q_x}, \eta_{q_y}) &= g(\xi_{q_x}, \eta_{q_y}) \quad \text{and} \\ g(\xi_{q_x}, \eta_{q_y + Q_y}) &= g(\xi_{q_x}, \eta_{q_y}), \end{aligned} \quad (27)$$

which are valid for all integers  $q_x$  and  $q_y$ . Because of the normalization condition of Eq. (9),

$$|g(\xi, \eta)| \leq 1 \quad (28)$$

for all  $\xi$  and  $\eta$ , with the equality holding only where the excitations interfere perfectly constructively. Therefore, when the field pattern is expressed in decibels, 0 dB corresponds to perfectly constructive interference.

## 6. PATTERN MEASURES

The code at the heart of the program analyzes the radiation pattern to obtain several measures that quantify the characteristics and performance of the array. The following subsections describe these measures, generally focusing on the concepts behind them and on their interpretation rather than on the specific method of calculation. Details of the algorithms and further discussion may be found in the code.

### 6.1. Pointing Vector, Pointing Error, and Peak Power Density

One of the most significant pattern measures is the direction of maximum radiation, here called the pointing vector. The program determines it directly from the field pattern and also indirectly from the excitations; the final pointing vector is a weighted average of the two, as discussed below. In identifying the pointing vector from the field pattern {563–787}, the program first locates the pattern's maximum magnitude over the grid of discrete direction cosines. For a well-formed beam, the neighboring samples should fall off parabolically, so they are fitted to the elliptic paraboloid<sup>13</sup>

$$|g(\xi, \eta)| = \frac{1}{2}U\xi^2 + W\xi\eta + \frac{1}{2}V\eta^2 + X\xi + Y\eta + Z \quad (29)$$

in a least-squares sense. If  $UV > W^2$ , as should be the case for a normal beam, the conic is indeed elliptical (corresponding to its level curves), and its maximum occurs at  $(\xi, \eta) = (p_{1x}, p_{1y})$ , where  $p_{1x}$  and  $p_{1y}$  satisfy

$$\begin{pmatrix} U & W \\ W & V \end{pmatrix} \begin{pmatrix} p_{1x} \\ p_{1y} \end{pmatrix} + \begin{pmatrix} X \\ Y \end{pmatrix} = \begin{pmatrix} 0 \\ 0 \end{pmatrix}. \quad (30)$$

The coordinate pair  $(p_{1x}, p_{1y})$  is taken to be the pointing vector for the first method. The deviation of the pattern samples from conic form is used to construct a covariance ellipse for  $p_{1x}$  and  $p_{1y}$  that expresses the uncertainty in their values.

The second method determines the pointing vector from the complex excitations {789–961}. Because a well-behaved array will have a nearly flat phase front, the excitation phases  $\Phi_{n_x, n_y}$  are fit to the plane  $-kn_x d_x \xi - kn_y d_y \eta - \Phi_0$ , weighted according to the excitation magnitudes. The pointing vector coordinates  $(p_{2x}, p_{2y})$  are the direction cosines  $(\xi, \eta)$  that give the best fit. As with the first method, a covariance ellipse for  $p_{2x}$  and  $p_{2y}$  is obtained from a measure of the deviation from the plane.

Each method is useful but limited. The first, the fit of the transform, is robust even for poorly aimed and malformed beams, but it is limited by the resolution of the Fourier transform. The second, the fit of the excitations, is independent of transform resolution but accurate only for nearly planar phase fronts, approaching the exact solution as the phase and time errors and quantization intervals decrease. To obtain a single pointing vector  $(p_x, p_y)$ , the program averages pointing vectors from the two methods, weighting each by the inverse of the area of its covariance ellipse {963–990}. An average covariance ellipse is also constructed in a consistent manner.

With the final pointing vector in hand, the pointing error  $\gamma$  is straightforwardly obtained {992–1046} from

$$\begin{aligned} \cos \gamma &= \mathbf{s} \cdot \mathbf{p} \\ &= s_x p_x + s_y p_y + s_z p_z, \end{aligned} \quad (31)$$

where  $s_z$  and  $p_z$  follow from unit magnitude constraints on  $\mathbf{s}$  and  $\mathbf{p}$ . If one desires the uncertainty in  $\gamma$  due to uncertainty in  $\mathbf{p}$ , an alternate calculation based on

$$\sin \gamma = |\mathbf{s} \times \mathbf{p}| \quad (32)$$

may be selected in the program.

The peak power density

$$P_{\max} = |g(p_x, p_y)|^2 \quad (33)$$

is calculated directly from Eq. (25).

## 6.2. Main Beam Region

The main beam region is the set of field pattern samples that are judged to belong to the main beam. Although normally not of interest as a final measure, it is essential for obtaining subsequent measures. It may be constructed conceptually by imagining a contour at an adjustable level. Beginning at the pattern maximum, we decrease the level so that the contour expands in size, following the topology of the main beam. Eventually the contour will intersect a local minimum or a saddle point; the closed contour about the pattern maximum at that level delineates the main beam region inside from the sidelobe region outside. Equivalently, that contour is the lowest one containing the global maximum that encircles no other local maxima. The power level of the contour is called the beam depth. Generally, well-formed beams are deep (that is, the beam depth is much less than one), while malformed beams are shallow, but the user should keep in mind that the beam depth depends on the transform resolution. In the program {1048–1137}, the beam depth is stored in the variable `beamDepthDB` in decibels relative to  $P_{\max}$  and is output to the user. Information obtained while determining the main beam region is used in finding the main beam width and roll, below, and the region itself is used directly in calculating the powers radiated into the main beam and sidelobes.

## 6.3. Main Beam Width and Roll

The level contours of the main beam generated by a two-dimensional array are nominally ellipses;<sup>14,15</sup> therefore they can be described by their center location, major and minor axes, and orientation. Having already obtained a measure of the beam's location in the form of the pointing vector, we use the major and minor axes and orientation of the elliptical contour at a given power level to describe the beam's shape {1139–1403}. The conventional power level is  $P_{\max}/2$ , or about 3 dB down. The angle subtended by the ellipse's longest diameter — its major axis — is taken as the beam's major width (that is, full width at half maximum power); that subtended by its shortest diameter, the beam's minor width. The ellipse orientation gives the roll angle, but we must choose an origin for the orientation angle. Construct three great circles as in Figure 4: *A*, along the azimuth reference; *B*, connecting boresight and the pointing vector; and *C*, along the beam's major width. The roll angle is defined as the sum of the angle between *A* and *B* and that between *B* and *C*. It happens that the roll angle so defined is merely the orientation of the major width relative to the azimuth reference when viewed in the stereographic projection, which preserves angles between great circles. Moreover, because the great circles along the beam's major and minor widths intersect orthogonally on the hemisphere, their stereographic projections do also. These facts motivate the program's use of stereographic coordinates for fitting an ellipse to the level contour and determining its major and minor axes and orientation. However, the roll angle and beam widths thereby obtained are approximate for two reasons. First, for beams off boresight, the great circles along the major and minor widths project as circles, whereas the major and minor axes of the projected ellipse are straight line segments. Second, the local scale in the projection increases away from boresight, artificially enlarging the portion of the beam farthest from boresight.<sup>12</sup> The error may become significant for beams far from boresight. A more sophisticated method of determining the beam widths is suggested near the end of the program code.

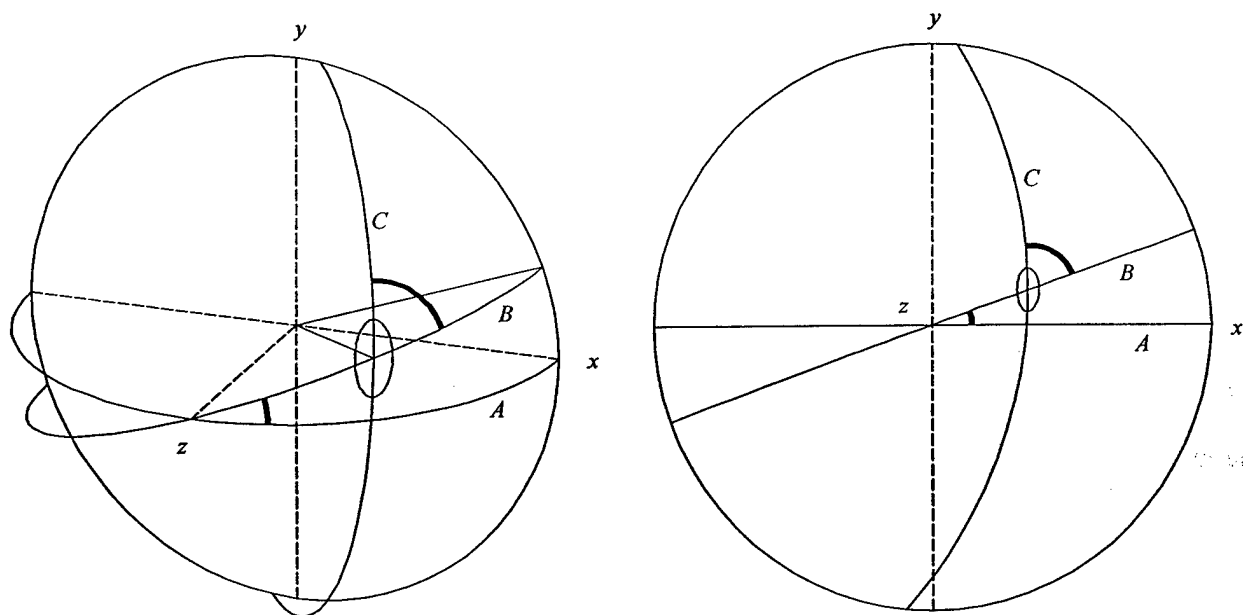


Figure 4 — Beam width ellipse and roll angle. The great circles  $A$ ,  $B$ , and  $C$  are described in the text, and the angles between them, indicated with thick arcs, are added to obtain the roll angle. The left projection is orthographic; the right, stereographic. The spherical coordinates of the pointing vector are  $\theta = 40^\circ$  and  $\psi = 20^\circ$ , the beam's major and minor widths are  $16^\circ$  and  $8^\circ$ , and the roll angle is  $90^\circ$ .

#### 6.4. Directivity, Power Ratios, and Average Sidelobe Level

The next measures obtained all depend on integrals of the power pattern over solid angle regions {1405–1527}. The integrals are calculated from the discrete samples of the pattern using the midpoint approximation, as detailed in the code. The solid angle regions of interest are visible space (the half-space  $z > 0$ ); the main beam, as described by the main beam region, above; and the sidelobes, defined as all regions of visible space not in the main beam. The program determines the total powers radiated into these regions; call them  $\Pi_v$  for visible space,  $\Pi_m$  for the main beam, and  $\Pi_s$  for the side lobes. We have

$$\Pi_v = \Pi_m + \Pi_s. \quad (34)$$

The directivity is the ratio of maximum to average power densities, assuming no back radiation into  $z < 0$ :

$$D = \frac{P_{\max}}{\Pi_v / 4\pi}. \quad (35)$$

The program also calculates the power ratios  $\Pi_m / \Pi_v$ ,  $\Pi_m / \Pi_s$ , and  $\Pi_v / \Pi_s$ , which generally decrease as the beam degrades. Finally, the average sidelobe level relative to the beam peak is

$$L_{\text{avg}} = \frac{\Pi_s}{\Omega_s P_{\max}}, \quad (36)$$

where  $\Omega_s$  is the solid angle occupied by the sidelobes.

## 6.5. Powers and Distances of Largest and Nearest Sidelobes

The last analysis identifies the sidelobe with the largest power density and the sidelobe closest to the main beam, and for each it reports the power density and angular distance from the main beam {1529–1677}. The power levels and locations of the sidelobes are obtained by fitting to elliptic paraboloids (Eq. (29)), and the power levels are reported relative to the beam peak  $P_{\max}$ .

## 7. MULTIPLE REALIZATIONS AND PARAMETER VALUES

The analyses described above apply to the radiation pattern corresponding to a single set of array parameters and one realization of any random variables. ARRSTATS contains two outer loops with which it analyzes multiple radiation patterns; one is a loop over realizations of random variables, and the other loops over a user-selected independent variable. The loop over realizations {190–218, 521–523, 1679–1819, 1905} is motivated by the following: When simulating random errors, one is usually interested not in the performance obtained by one realization of the errors but rather in the performance statistics for an ensemble of statistically identical arrays. To that end, ARRSTATS can generate an arbitrary, user-specified number of realizations for which it will accumulate performance statistics. The program outputs the mean and standard deviation of each performance measure. The second loop {175–188, 326–336, 2578–2579}, over an independent variable, allows the user to examine the variation of performance measures as the variable changes. Possible independent variables include but are not limited to the operating and reference frequencies, steering angles, error parameters, quantization intervals, and even parameters of the array geometry. ARRSTATS produces a graph showing each measure as a function of the independent variable, as discussed below.

## 8. PROGRAM OUTPUT

ARRSTATS outputs its results in three ways: textual output of running statistics, a plot of the radiation pattern for the last realization in an ensemble, and a summary plot of the performance measures as functions of the independent variable. The textual output is a table like that in Fig. 5 printed to the MATLAB command window {1864–1903}. The values in the table are the means and standard deviations of the performance measures for all members of the statistical ensemble that have been realized thus far. The table may be interpreted according to the descriptions in Section 6, keeping in mind the following.

```
Means and [std devs] for 16 of 16 realizations
beam direction : (29.954, 60.007) deg, std dev 0.038 deg
pointing error : 0.0528 [0.0279] deg
peak power dens: -0.426 [0.034 ] dB
beam depth : -24.66 [1.49 ] dB re peak
beam width : ( 2.095 [0.005 ], 1.813 [0.004]) deg
beam roll : 59.56 [0.65 ] deg
directivity : 38.894 [0.034 ] dB
power ratio m/v: -1.360 [0.030 ] dB
power ratio m/s: 4.347 [0.113 ] dB
power ratio v/s: 5.707 [0.083 ] dB
avg sidelobe : -41.61 [0.11 ] dB re peak
nrst sidelobe : -13.16 [0.69] dB re peak, 3.00 [0.01] deg off beam
lgst sidelobe : -12.30 [0.58] dB re peak, 3.11 [0.09] deg off beam
```

Figure 5 — Textual output of running statistics. The parameters of this example are in the code listing; for the values above, the standard deviation of the subarray time error is 10 ps (stdTimeMPS = 10).



The coordinates specifying the beam direction are the spherical coordinates ( $\theta$  and  $\psi$ ) of the average pointing vector {1821–1862}. The standard deviation of the beam direction is an estimate of the rms angular deviation of the ensemble of pointing vectors from their mean {1821–1862}. Both the beam direction coordinates and roll angle include compensation for the azimuth offset *azmthOffst*. The peak power density is relative to perfectly constructive interference, and the beam depth, average sidelobe level, and levels of the nearest and largest sidelobes are relative to the peak power density (suggested by the use of “dB re peak” in the table).

To aid in visualizing an array’s performance, ARRSTATS can graphically present the radiation pattern and several of the performance measures as in Fig. 6 {220–324, 2138–2574}. A significant

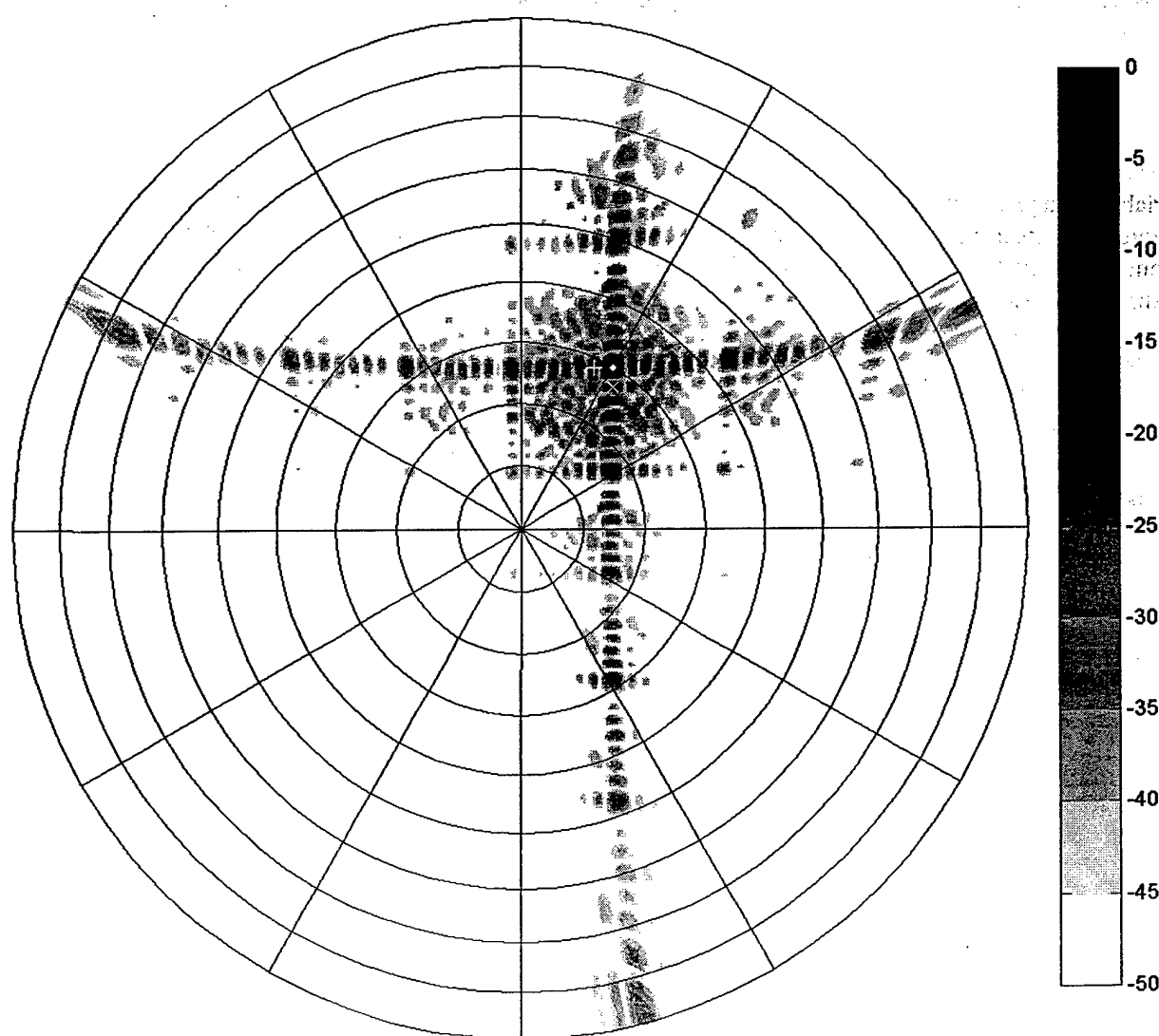


Figure 6 — Lambert projection of the radiation pattern with a spherical coordinate grid superimposed. Boresight is at the center, and the steering vector is ( $\theta = 30^\circ$ ,  $\psi = 60^\circ$ ). The white dot denotes the beam peak;  $\times$ , the largest sidelobe; and  $+$ , the nearest sidelobe. The legend gives the power in dB relative to perfectly constructive interference. The pattern is one realization of the case *stdTimeMPS* = 10 for the parameters given in the code listing.

plotting option is the choice of projection from among those described in Section 2. Briefly, the Lambert projection preserves the relative areas of regions (for example, the size of the main beam relative to the hemisphere or to prominent sidelobes), the stereographic projection preserves local shape (and the orthogonality of the major and minor beam width cuts), and the orthographic projection gives a picture of the hemisphere. The pattern may be plotted linearly or logarithmically in power, and the logarithmic depth may be specified. The user may also specify the color map and shading method to use. The performance measures that can be graphically indicated on the radiation pattern include the pointing vector, the axes of the uncertainty ellipse of the pointing vector, the actual and fitted beam width contours, the main beam region, the locations of the nearest and largest sidelobes, and other measures of less frequent interest. If multiple realizations are generated, the radiation pattern will be plotted only for the last realization as a representative of the ensemble.

If the outer loop over an independent variable is used, the summary figure plots the performance measures as functions of the independent variable, as in Fig. 7 {220–324, 1907–2136}. The figure groups fifteen measures (all except the beam direction) into eight subplots and utilizes distinct colors or line styles and both left and right axes for the ordinates. The title of each subplot gives the names of the measures; where multiple colors or linestyles appear, each measure name is followed by a color or style code in parenthesis, and where left and right axes are used, an axis code (“L” or “R”) also appears. If more than one realization was generated for each value of the independent variable, error bars extend one standard deviation above and one standard deviation below each point.

## 9. SUMMARY

We have introduced a computer program for assessing the effects of errors in rectangular-grid planar array antennas. The most general array comprises phase-steered elements grouped into time-steered subapertures and subarrays; this includes strictly phase-steered arrays and time-steered arrays as particular cases. The time and phase delays may be quantized, and random errors may be assigned to the times, phases, and amplitudes. From simulated radiation patterns, the program obtains performance measures over statistical ensembles and as functions of a user-specified independent variable, producing textual and graphical output.

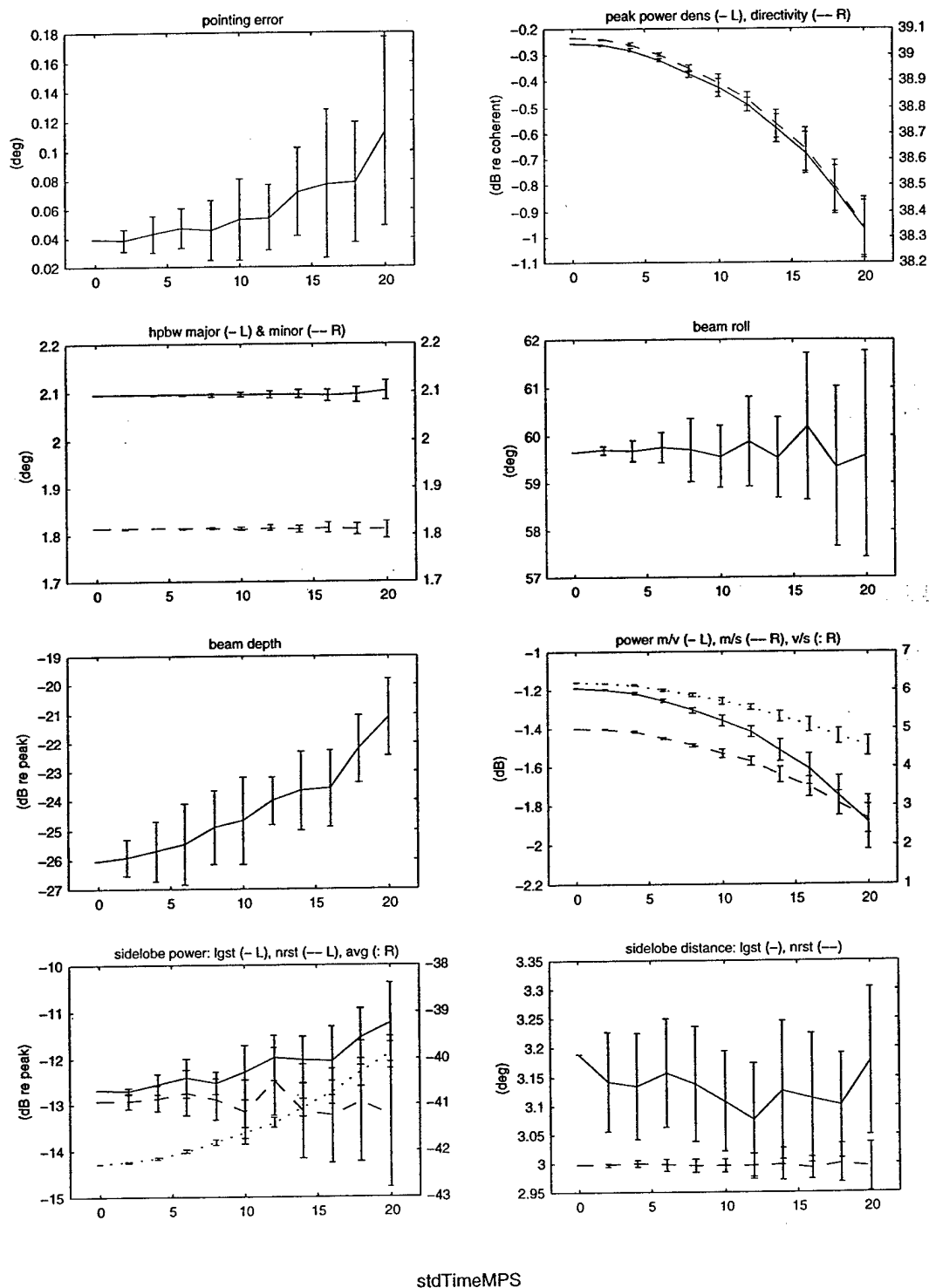


Figure 7 — Summary plots. This example shows the degradation of performance as the standard deviation of the subarray time error ( $\text{stdTimeMPS}$ , in picoseconds) increases. The parameters of the run may be found in the code listing.

## Appendix A

### LIST OF VARIABLES

This list of significant variables mentioned in this report gives their symbol in this report, coded name, and description. It does not include all program variables. Ellipses (...) stand for prefixes, and asterisks (\*) indicate that the variable holds the specified quantity temporarily.

Text	Code	Description
$x, y, z$		coordinates in real space
$\xi, \eta, \zeta$	dirCosX, ...Y, ...Z	direction cosines
$s_x, s_y$	sX, sY	steering vector direction cosines
$\theta$	...Polar	spherical polar coordinate
$\psi$	...Azmth	spherical azimuth coordinate
$\alpha$	...Az	traditional azimuth coordinate
$\varepsilon$	...El	traditional elevation coordinate
$r$		radial coordinate of projection
$d_x, d_y$	dx, dy	element spacings
$L_x, L_y$	numLX, numLY	numbers of subapertures
$M_x, M_y$	numMX, numMY	numbers of subarrays per subaperture
$N_x, N_y$	numNX, numNY	numbers of elements per subarray
$l_x, l_y$	lx, ly	subaperture labels
$m_x, m_y$	mx, my	subarray labels
$n_x, n_y$	nx, ny	element labels
	diamond	indicates diamond element pattern
	azmthOffst	antenna rotation angle about boresight
$f_0$	fRef	reference frequency
$f$	fOpr	operating frequency
$k_0$		reference wave number
$k$		operating wave number
$\omega_0$		reference angular frequency
$\omega$		operating angular frequency
$\sigma_R$	stdAmplL	standard deviation of subaperture amplitude error
$\sigma_r$	stdAmplM	standard deviation of subarray amplitude error
$\sigma_p$	stdAmplN	standard deviation of element amplitude error
$R$		random subaperture amplitude error
$r$		random subarray amplitude error

Text	Code	Description
$\rho$		random element amplitude error
$\bar{a}$	excMagIdl	error-free (ideal) excitation magnitude
$a$	excMag	erroneous (actual) excitation magnitude
$\delta T$	qntTimeL	subaperture time quantization interval
$\delta t$	qntTimeM	subarray time quantization interval
$\delta \phi$	qntPhseN	element phase quantization interval
$\Delta T_x, \Delta T_y$		subaperture time steps
$\Delta t_x, \Delta t_y$		subarray time steps
$\Delta \phi_x, \Delta \phi_y$		element phase steps
$T_{n_x n_y}$	TimeL*	error-free subaperture time delays
$t_{n_x n_y}$	TimeM*	error-free subarray time delays
$\phi_{n_x n_y}$	PhseN*	error-free element phase delays
$\hat{T}_{n_x n_y}$	TimeL	quantized subaperture time delays
$\hat{t}_{n_x n_y}$	TimeM	quantized subarray time delays
$\hat{\phi}_{n_x n_y}$	PhseN	quantized element phase delays
$\sigma_T$	stdTimeL	standard deviation of subaperture time error
$\sigma_t$	stdTimeM	standard deviation of subarray time error
$\sigma_\phi$	stdPhseN	standard deviation of element phase error
$\mathcal{T}$	ofsTimeL	deterministic subaperture time error
$\tilde{T}$		random subaperture time error
$\tilde{t}$		random subarray time error
$\tilde{\phi}$		random element phase error
$\bar{\Phi}$		error-free excitation phase
$\hat{\Phi}$	excPhsIdl	quantized excitation phase
$\tilde{\Phi}$	excPhsErr	excitation phase error
$\Phi$	excPhs	erroneous (actual) excitation phase
$g$	g	field pattern
$Q_x, Q_y$	tx, ty	number of points in Fourier transform
$p_x, p_y$	px, py	pointing vector direction cosines
$\gamma$	errPoint	pointing error
$P_{\max}$	gSqrMax	maximum power density
$L_{\text{avg}}$	powerSideAvgDB	average relative sidelobe level ( $\text{powerSideAvgDB} = 10 \log_{10} L_{\text{avg}}$ )
$\Pi_v$	powerVisb	power radiated into visible space
$\Pi_m$	powerMain	power radiated into the main beam
$\Pi_s$	powerSide	power radiated into the side lobes
$D$	directivityDB	directivity ( $\text{directivityDB} = 10 \log_{10} D$ )

## Appendix B

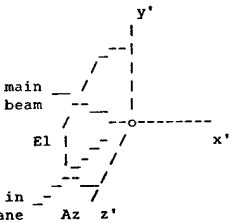
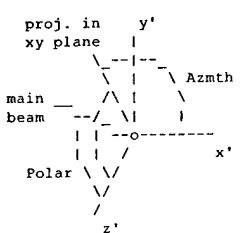
### PROGRAM LISTING

```

1  % Calculate performance parameters of an array with excitation errors
2  %
3  % The excitation time and phase convention is exp (-i (omega t + phi));
4  % positive (negative) phases phi correspond to a leading (lagging)
5  % excitation. Distances are stored in meters; times, nanoseconds;
6  % frequencies, gigahertz. Angles (both geometric and phase) are always
7  % specified in radians. Generally, the coordinate x increases with the
8  % column index; y, with the row index.
9  %
10 % Parameters that may be changed by the user are marked "INPUT" in
11 % comments. Frequently-used inputs appear near the top of the program,
12 % but some inputs are defined elsewhere, particularly in the plotting
13 % section.
14 %
15 % Suggestions for improvements are provided at the end of the program.
16 %
17 % This program is coded for Matlab version 5.3 (Release 11), although
18 % most of the code will run under version 4.2.
19 %
20 % Written by Stan West, 1998, 1999
21 % U.S. Government work not subject to copyright
22 %
23 % Declare physical and conversion constants
24 %
25 c = 0.299792458; % speed of light in m/ns
26 rpd = pi / 180; % radians per degree
27 twopi = 2 * pi;
28 %
29 % Set operating frequency relative to reference frequency
30 %
31 % At the reference frequency, or fOpr = fRef, the time and phase delays
32 % will properly steer the antenna in the absence of error and
33 % quantization.
34 %
35 fRef = 3.0; % INPUT reference frequency in GHz
36 fOpr = fRef + 1 * 0.5 / 2; % INPUT operating frequency in GHz
37 % center frequency + {-1 ... 1} * bandwidth / 2
38 %
39 % Describe array geometry and error statistics
40 %
41 % Elements lie on a regular planar grid and are grouped heirarchically.
42 % The array is subdivided into numLX subapertures in the x dimension and
43 % numLY subapertures in the y dimension. Each subaperture is
44 % time-steered and has associated with it a user-set deterministic
45 % absolute time error, a random absolute time error, and a random
46 % relative amplitude error. The random errors are normally-distributed
47 % with zero mean and user-set standard deviation. Each subaperture
48 % contains numMX by numMY subarrays, each of which, like the
49 % subapertures, is time-steered and has a random absolute time error and
50 % a random relative amplitude error. Finally, each subarray contains
51 % numNX by numNY elements, each of which is phase-steered and has a
52 % random absolute phase error and a random relative amplitude error.
53 % All elements are spaced by dx in x and dy in y, even across subarrays
54 % and subapertures.
55 %
56 % Set parameters of subapertures
57 %
58 numLX = 1; % INPUT number of subapertures in x
59 numLY = 1; % and y dimensions
60 qntTimeL = 0; % INPUT quantization interval in ns; 0 for no quantization
61 ofsTimeL = zeros (numLY, numLX); % INPUT deterministic absolute time error in each subaperture in ns
62 stdTimeL = 0.000; % INPUT standard deviation of absolute time error in each subaperture in ns
63 stdAmpLL = 0.0; % INPUT standard deviation of relative amplitude error
64 %
65 % Set parameters of subarrays
66 %
67 numMX = 8; % INPUT number of subarrays in x
68 numMY = 8; % and y dimensions per subaperture
69 qntTimeM = 0; % INPUT quantization interval in ns; 0 for no quantization
70 stdTimeM = 0.00; % INPUT standard deviation of absolute time error in each subarray in ns
71 stdAmpLM = 0.0; % INPUT standard deviation of relative amplitude error
72 %
73 % Set parameters of elements
74 %
75 dx = 1.6 * 0.0254; % INPUT element spacing in x

```

```

76 dy = 1.6 * 0.0254; % and y dimensions in meters
77 numNX = 8; % INPUT number of elements in x
78 numNY = 8; % and y dimensions per subarray
79 qntPhseN = 0 * rpd; % INPUT quantization interval in radians; 0 for no quantization
80 stdPhseN = 0 * rpd; % INPUT standard deviation of absolute phase error in each element in radians
81 stdAmpN = 0.0; % INPUT standard deviation of relative amplitude error
82 %
83 % Set other parameters
84 %
85 diamond = 0; % INPUT 0: full array; 1: eliminate excitations on even diagonals
86 azmthOffst = 0 * rpd; % INPUT angle of the positive x axis of the array above the azimuth reference
87 %
88 % Alternatively, select an array
89 %
90 switch 0 % INPUT case number for arrays below or 0 to use values above
91 case 1
92 % Insert frequency, array, and error parameters here
93 case 2
94 end
95 %
96 % Specify steering angle
97 %
98 % Two coordinate systems, described below, are available for specifying
99 % the steering angle: traditional azimuth/elevation coordinates and
100 % spherical coordinates. Azimuth/elevation coordinates are converted to
101 % spherical coordinates for internal program use, and output is given in
102 % spherical coordinates.
103 %
104 % In the diagrams below, the antenna lies in the x'-y' plane with
105 % boresight along the positive z' axis. The antenna's z axis coincides
106 % with z', and its x axis is at an angle azmthOffst above the x' axis,
107 % which is the azimuth reference.
108 %
109 % The equations relating the the Cartesian coordinates x', y', and z' of
110 % a unit vector, the spherical coordinates Polar and Azmth, and the
111 % traditional coordinates Az and El are
112 %
113 %  $x' = \sin \text{Polar} \cos \text{Azmth} = -\cos \text{El} \sin \text{Az}$ 
114 %  $y' = \sin \text{Polar} \sin \text{Azmth} = \sin \text{El}$ 
115 %  $z' = \cos \text{Polar} = \cos \text{El} \cos \text{Az}$ 
116 %
117 %  $\cos \text{Polar} = \cos \text{El} \cos \text{Az} = z'$ 
118 %  $\tan \text{Azmth} = -\tan \text{El} / \sin \text{Az} = y' / x'$ 
119 %
120 %  $-\tan \text{Az} = \tan \text{Polar} \cos \text{Azmth} = x' / z'$ 
121 %  $\sin \text{El} = \sin \text{Polar} \sin \text{Azmth} = y'$ 
122 %
123 % Since (x', y', z') is a unit vector, its components are direction
124 % cosines.
125 %
126 switch 2
127 case 1
128 %
129 % 
130 % Use azimuth/elevation
131 % coordinates. Given the
132 % projection of the steering vector
133 % onto the x'-z' plane, the azimuth
134 % is the angle between it and the
135 % z' axis, while the elevation is
136 % the angle between it and the
137 % steering vector. In the diagram,
138 % both angles are positive.
139 %
140 %
141 %  $\text{steerAz} = 30 * \text{rpd};$  % INPUT azimuth angle
142 %  $\text{steerEl} = 30 * \text{rpd};$  % INPUT elevation angle
143 %  $\text{steerPolar} = \text{acos}(\cos(\text{steerEl}) * \cos(\text{steerAz}));$ 
144 %  $\text{steerAzmth} = \text{atan2}(\tan(\text{steerEl}), -\sin(\text{steerAz}));$ 
145 %
146 case 2
147 %
148 % 
149 % Use spherical coordinates. The
150 % polar angle is the angle
151 % between the z' axis and the
152 % steering vector. The azimuth
153 % angle is the angle between the
154 % x' axis and the projection of
155 % the steering vector onto the
156 % x'-y' plane. In the diagram,
157 % both angles are positive.
158 %
159 %
160 %  $\text{steerPolar} = 30 * \text{rpd};$  % INPUT polar angle
161 %  $\text{steerAzmth} = 60 * \text{rpd};$  % INPUT azimuth angle
162 %
163 otherwise
164 error('Invalid switch parameter.');
```

end

```

166 steerAzmth = steerAzmth - azmthOffst; % now relative to antenna's x axis
167
```

```

168 % Set transform size
169 %
170 % (See comments elsewhere related to the discrete Fourier transform.)
171 %
172 tx = 2^9; % INPUT number of transform points in x
173 ty = 2^9; % and y
174
175 % Declare independent variable and its values
176 %
177 % The main loop iterates over values of the independent variable named
178 % below. The independent variable may be any parameter, including, for
179 % example, those describing geometry, frequency, error, quantization,
180 % and steering angle. It may also be an otherwise unknown variable that
181 % is transformed to a known program parameter by custom code in the main
182 % loop. To effectively disable the loop, set a dummy variable to a
183 % scalar value.
184 %
185 indVarName = 'stdTimeMPS'; % INPUT name of independent variable
186 indVar = 0 : 2 : 20; % INPUT vector of values it will assume
187 indVar = indVar (:); % make it a column vector
188 indVarLen = length (indVar);
189
190 % Initialize statistics variables
191 %
192 % If the excitations are random, one is often interested in the mean and
193 % standard deviation of the performance measures. For each value of the
194 % independent variable, the program will generate numRiz realizations of
195 % the random excitations and accumulate the statistics of the
196 % performance measures.
197 %
198 numRiz = 16; % INPUT number of realizations to generate
199 numAcc = nan * ones (indVarLen, 1); % number of realizations accumulated
200 pxS = nan * ones (indVarLen, 2);
201 pyS = nan * ones (indVarLen, 2);
202 pzS = nan * ones (indVarLen, 2);
203 errPoints = nan * ones (indVarLen, 2);
204 % errPointUncS = nan * ones (indVarLen, 2); % see later calculation of pointing error
205 beamPowerDBS = nan * ones (indVarLen, 2);
206 beamDepthDBS = nan * ones (indVarLen, 2);
207 hpbwMjrs = nan * ones (indVarLen, 2);
208 hpbwMnrs = nan * ones (indVarLen, 2);
209 rolls = nan * ones (indVarLen, 2);
210 directivityDBS = nan * ones (indVarLen, 2);
211 powerMainVisbDBS = nan * ones (indVarLen, 2);
212 powerMainSideDBS = nan * ones (indVarLen, 2);
213 powerVisbSideDBS = nan * ones (indVarLen, 2);
214 powerSideAvgDBS = nan * ones (indVarLen, 2);
215 slNrstDistS = nan * ones (indVarLen, 2);
216 slNrstPowrDBS = nan * ones (indVarLen, 2);
217 slLgstDistS = nan * ones (indVarLen, 2);
218 slLgstPowrDBS = nan * ones (indVarLen, 2);
219
220 % Initialize graphics
221 %
222 cmap = jet; % INPUT color map
223 invertBkgd = 0; % INPUT 0: figure background is lowest value of the colormap;
224 % 1: " highest
225 sumBW = 0; % INPUT 0: summary plot in color; 1: in black and white
226 figPat = 1; % INPUT figure number for power pattern
227 figSum = 2; % and summary
228 cbarVert = 0; % INPUT 0 for horizontal bar below pattern, 1 for vertical to right
229 %
230 % Set window positions
231 %
232 cbarSize = 0.15; % colorbar size relative to pattern
233 marginWid = 8; % width margin in pixels
234 marginHgt = 44; % height margin in pixels
235 screenSize = get (0, 'screenSize');
236 screenWid = screenSize (3);
237 screenHgt = screenSize (4);
238 figPatWid = 0.45 * (screenSize (3) - 4 * marginWid); % width of pattern figure
239 figSumWid = screenSize (3) - 4 * marginWid - figPatWid; % width of summary figure
240 if cbarVert
241 figPatHgt = figPatWid; % height of pattern figure
242 figPatWid = figPatWid * (1 + cbarSize);
243 else
244 figPatHgt = figPatWid * (1 + cbarSize);
245 end
246 figure (figPat); % create and position pattern figure
247 figPat = gcf; % update in case figPat couldn't be created
248 set (figPat, ...
249 'position', [marginWid
250 screenHgt-marginHgt-figPatHgt ...
251 figPatWid ...
252 figPatHgt], ...
253 'paperUnits', 'inches')
254 if cbarVert
255 set (figPat, ...
256 'PaperOrientation', 'landscape', ...
257 'PaperPosition', [0.5 0.5 10 7.5]);
258 else
259 set (figPat, ...

```



```

260     'PaperOrientation', 'portrait', ...
261     'PaperPosition', [0.5 0.5 7.5 10]);
262 end
263 clf;
264 figure (figSum); % create and position summary figure
265 figSum = gcf; % update in case figSum couldn't be created
266 set (figSum, ...
267     'position', [screenWid-marginWid-figSumWid ...
268                 marginHgt ...
269                 figSumWid ...
270                 screenHgt-2*marginHgt]);
271 orient tall;
272 clf;
273 %
274 % Set pattern figure colors
275 %
276 if invertBkgd
277     bkgd = cmap (size (cmap, 1), :); % take background from high...
278 else
279     bkgd = cmap (1, :); % or low end of colormap
280 end
281 whitebg (figPat, bkgd); % set pattern colors
282 set (figPat, 'color', bkgd); % override default background of whitebg
283 %
284 % Set summary figure colors and linestyles
285 %
286 whitebg (figSum, 'w'); % set summary colors
287 set (figSum, 'color', 'w'); % override default background of whitebg
288 if sumBW
289     discrim = 'lineStyle';
290     discrimValue = {'-'; '--'; ':'}; % line styles
291     discrimName = discrimValue; % names for legends will be same as style codes
292     set (figSum, ... % black color forces cycling through line styles
293         'DefaultAxesLineStyleOrder', discrimValue, ...
294         'DefaultAxesColorOrder', [0 0 0]);
295 else
296     discrim = 'color';
297     set (figSum, ... % reset (if previously b&w, for
298         'defaultAxesColorOrder', 'default', ... % example)
299         'defaultAxesLineStyleOrder', 'default');
300     discrimValue = get (figSum, 'defaultAxesColorOrder'); % put colors in array of RGB coordinates
301     colorOrderHSV = rgb2hsv (discrimValue); % equivalent HSV coordinates
302     discrimValue = num2cell (discrimValue, 2); % put each row in a cell
303     colorNames = {'RYGCBMKW'}; % first six by hue, then black & white
304     discrimName = colorNames (1 + ... % convert H to an integer 0..5
305         mod (round (6 * colorOrderHSV (:, 1)), 6)); % then index into colorNames
306     unsat = find (colorOrderHSV (:, 2) <= 0.25); % unsaturated (gray) colors
307     if ~isempty (unsat)
308         discrimName (unsat) = colorNames (7 + ... % threshold V to 0 (K) or 1 (W)
309             (colorOrderHSV (unsat, 3) > 0.5)); % then index into colorNames
310     end
311     discrimName = cellstr (discrimName); % put each letter in a cell
312     clear colorOrderHSV colorNames unsat;
313 end
314 %
315 % Set miscellaneous common properties
316 %
317 set ([figPat figSum], ...
318     'invertHardCopy', 'off', ...
319     'defaultFontSize', 8, ...
320     'defaultAxesFontSize', 8, ...
321     'toolbar', 'none');
322 drawnow;
323 clear marginWid marginHgt screenSize screenWid screenHgt;
324 clear figPatWid figSumWid figPatHgt bkgd;
325 %
326 % Loop over independent variable
327 %
328 for indx = 1 : indVarLen
329     %
330     % Set value of independent variable
331     %
332     eval ([indVarName ' = indVar (indx);']); % set variable to value
333     %
334     % Code may be inserted below to transform the independent variable to
335     % known program variables.
336     stdTimeM = stdTimeMPS * 1e-3;
337     %
338     % Define labels for substructures
339     %
340     % Here we construct row and column vectors (corresponding to x and y,
341     % respectively) that tell to which subaperture, subarray, or element a
342     % given position corresponds. The sample vectors are for numLX =
343     % numLY = 2, numMX = numMY = 3, and numNX = numNY = 2.
344     %
345     numLMX = numLX * numMX; % total number of subarrays
346     numLMY = numLY * numMY;
347     numLMNX = numLMX * numNX; % total number of elements
348     numLMNY = numLMY * numNY;
349     nx = 0 : numLMNX - 1; % e.g., [0 1 2 3 4 5 6 7 8 9 10 11]
350     ny = (0 : numLMNY - 1)'; % [0 1 2 3 4 5 6 7 8 9 10 11]'
351     mx = floor (nx / numNX); % [0 0 1 1 2 2 3 3 4 4 5 5]

```

```

352 my = floor (ny / numNY); % [0 0 1 1 2 2 3 3 4 4 5 5]'
353 lx = floor (nx / (numMX * numNX)); % [0 0 0 0 0 0 1 1 1 1 1 1]'
354 ly = floor (ny / (numMY * numNY)); % [0 0 0 0 0 0 1 1 1 1 1 1]'
355
356 % Calculate ideal (error-free) excitation magnitudes
357 %
358 excMagIdl = ones (numLMNY, numLMNX); % uniform weighting
359 if diamond % zero every other element
360 excMagIdl = excMagIdl ...
361 .* rem (ones (numLMNY, 1) * nx + ny * ones (1, numLMNX), 2);
362 end
363 excMagIdl = excMagIdl / sum (excMagIdl(:).^2); % normalize to unit power
364
365 % Calculate ideal (error-free) excitation phases
366 %
367 % The ideal excitation phases are those that produce perfectly
368 % constructive interference in the direction of the steering vector at
369 % the reference frequency. This implies a linear phase progression
370 %
371 excPhsIdl = -k0 (dx sx nx + dy sy ny) + const.,
372 %
373 % where k0 (= 2 pi fRef) is the reference wave vector. Quantization
374 % prevents the array from achieving this flat phase front for all
375 % steering angles. However, the beamformer simulated here mitigates
376 % effects due to subaperture quantization by adjusting the subarray
377 % delays, which is effective if the subarrays are quantized at a finer
378 % interval than the subapertures. Likewise, it compensates for
379 % subarray quantization with the element phasers.
380 %
381 % We choose the constant in the phase progression to be zero, which
382 % means that the lowest and leftmost components (those for which lx,
383 % ly, mx, my, nx, or ny is zero) are never delayed, while the highest
384 % and rightmost components have delays that depend strongly on the
385 % steering vector.
386 %
387 sx = sin (steerPolar) * cos (steerAzimuth); % direction cosines
388 sy = sin (steerPolar) * sin (steerAzimuth); % for steering
389 sz = cos (steerPolar); % used much later
390 TimeLX = -dx * sx * numNX * numMX * lx / c;
391 TimeLY = -dy * sy * numNY * numMY * ly / c;
392 TimeL = ones (numLMNY, 1) * TimeLX + TimeLY * ones (1, numLMNX);
393 if qntTimeL ~= 0 % quantize?
394 TimeL = round (TimeL / qntTimeL) * qntTimeL; % yes
395 end;
396 TimeMX = -dx * sx * numNX * mx / c;
397 TimeMY = -dy * sy * numNY * my / c;
398 TimeM = ones (numLMNY, 1) * TimeMX + TimeMY * ones (1, numLMNX) - TimeL;
399 if qntTimeM ~= 0
400 TimeM = round (TimeM / qntTimeM) * qntTimeM;
401 end;
402 TimeNX = -dx * sx * nx / c;
403 TimeNY = -dy * sy * ny / c;
404 PhsEN = twopi * fRef * ...
405 (ones (numLMNY, 1) * TimeNX + TimeNY * ones (1, numLMNX) - TimeL - TimeM);
406 if qntPhsEN ~= 0
407 PhsEN = round (PhsEN / qntPhsEN) * qntPhsEN;
408 end;
409 excPhsIdl = twopi * fOpr * (TimeL + TimeM) + PhsEN;
410 clear TimeLX TimeLY TimeL TimeMX TimeMY TimeM TimeNX TimeNY TimeN PhsEN;
411
412 % Prepare transform mapping
413 %
414 % The far-field array factor is the Fourier transform of the complex
415 % excitations. Considering the x dimension only (the operation in the
416 % y dimension is analogous), the discrete Fourier transform (DFT) used
417 % later calculates the far-field array factor at the direction cosine
418 % cx as
419 %
420 % tx-1
421 % g (cx) = sum exp (-i k cx dx q) e ,
422 % q=0 q
423 %
424 % where the e[q] are the complex excitations (zero-padded if tx
425 % exceeds the array size), k (= 2 pi / lambda) is the operating wave
426 % vector, and lambda (= c / fOpr) is the operating wavelength. The
427 % argument of the exponential in the transform may be written -i 2 pi
428 % (cx / lambda) * (dx q), where cx / lambda is the spatial frequency
429 % and dx q is the spatial coordinate. The direction cosines for which
430 % g is calculated in the DFT are
431 %
432 % lambda p
433 % cx = -----, p = 0, 1, ..., tx - 1
434 % p dx tx
435 %
436 % so that the argument of the exponential is -i 2 pi p q / tx. We
437 % have
438 %
439 % g (cx) = g (cx) for any integer p.
440 % p+tx p
441 %
442 % Given g (cx[p]), the array factor may be obtained at any angle using
443 %

```

```

444 %          tx-1 / p   dx cx   \
445 %      g (cx) = sum S | -- - ---- , tx | g (cx )
446 %          p=0   \ tx   lambda /   p
447 %
448 % where the geometric progression
449 %
450 %          1 tx-1
451 %      S (x, tx) = -- sum exp (i 2 pi q x)
452 %          tx q=0
453 %
454 %          1 exp (i 2 pi x tx) - 1
455 %      = -----
456 %          tx exp (i 2 pi x) - 1
457 %
458 % is an interpolating function, but this formula is not used below.
459 % Incidentally, note that
460 %
461 %          1 | sin (tx pi x) |
462 %      |S (x, tx)| = -- | ----- | ,
463 %          tx | sin (pi x) |
464 %
465 % an expression that often appears in array theory.
466 %
467 % After the DFT is calculated, the program maps the results into the
468 % region of cx-cy space where the direction cosines have magnitude 1
469 % or less, tiling as necessary to fill the region. The portion of
470 % that region for which cx^2 + cy^2 <= 1 corresponds to visible real
471 % space (radiating waves). Later processing requires a border of at
472 % least one element outside the visible region. This section prepares
473 % the mapping.
474 %
475 % txLim = tx * dx * fOpr / c; % values of p (not necessarily
476 % tyLim = ty * dy * fOpr / c; % integer) for which cx and cy are 1
477 % txIndxLimMin = -floor (txLim) - 1; % largest integers p for which
478 % tyIndxLimMin = -floor (tyLim) - 1; % cx, cy > -1
479 % txIndxLimMax = floor (txLim + 0.5) + 1; % smallest integers p for which cx,
480 % tyIndxLimMax = floor (tyLim + 0.5) + 1; % cy > (1 + half element spacing)
481 % Extra half element spacing is needed only for surface plots with
482 % flat shading; see graphics code below
483 % ax = txIndxLimMax - txIndxLimMin + 1; % number of angle samples in x
484 % ay = tyIndxLimMax - tyIndxLimMin + 1; % and y
485 % txIndx = txIndxLimMin : txIndxLimMax ; % row vector of indices
486 % tyIndx = (tyIndxLimMin : tyIndxLimMax)'; % column vector
487 % dirCosX = txIndx / txLim; % corresponding direction cosines
488 % dirCosY = tyIndx / tyLim; % cx and cy
489 % dirCosShiftX = (txIndx - 0.5) / txLim; % shifted direction cosines for use
490 % dirCosShiftY = (tyIndx - 0.5) / tyLim; % with flat shading
491 % txIndx = txIndx - tx * floor (txIndx / tx); % zero-based indices into columns
492 % tyIndx = tyIndx - ty * floor (tyIndx / ty); % (x) and rows (y) of DFT results
493 % The above lines accomplish the tiling function by folding the
494 % indices into the interval [0, tx - 1]
495 % tIndx = tyIndx * ones (1, ax) ... % indices to elements (one-based,
496 % + ones (ay, 1) * txIndx * ty + 1; % column-ordered)
497 % clear txIndxLimMin tyIndxLimMin txIndxLimMax tyIndxLimMax txIndx tyIndx;
498 %
499 % Prepare far-field angle mapping
500 %
501 % Physically, the array factor is a function of position on a
502 % hemisphere. The direction cosines used in the Fourier transform are
503 % the x and y coordinates of points on the unit hemisphere. Below we
504 % determine the region of the transform results that corresponds to
505 % visible space, namely cx^2 + cy^2 <= 1, and calculate the z
506 % coordinates of points in visible space according to
507 %
508 %          2      2 1/2
509 %      cz = (1 - cx - cy) , Re cz >= 0.
510 %
511 % For points outside visible space, cz is set to zero.
512 %
513 % dirCosXmtx = ones (ay, 1) * dirCosX; % now a matrix
514 % dirCosYmtx = dirCosY * ones (1, ax);
515 % radSqr = dirCosXmtx.^2 + dirCosYmtx.^2; % squared radius
516 % visBool = logical (radSqr < 1); % 1 in visible space, 0 elsewhere
517 % dirCosZmtx = zeros (ay, ax); % 0 outside visible space
518 % dirCosZmtx (visBool) = sqrt (1 - radSqr (visBool)); % positive in visible space
519 % clear radSqr;
520 %
521 % Loop over realizations
522 %
523 % for r1zNum = 1 : numR1z
524 %
525 %     Calculate excitation magnitudes with error
526 %
527 %     excMagErr = 1 + stdAmplN * randn (numLMNY, numLMNX); % element-level error
528 %     err = 1 + stdAmplM * randn (numLMY, numLMX); % temporary matrix
529 %     excMagErr = excMagErr .* err (my + 1, mx + 1); % subarray-level error
530 %     err = 1 + stdAmplL * randn (numLY, numLX); % temporary
531 %     excMagErr = excMagErr .* err (ly + 1, lx + 1); % subaperture-level error
532 %     excMag = excMagErr .* excMagIdl; % actual (with error) magnitude
533 %     clear err excMagErr;
534 %
535 %     Calculate excitation phases with error

```

```

536 %
537 excPhsErr = stdPhseN * randn (numLMNY, numLMNX); % element-level error
538 err = stdTimeM * randn (numLMY, numLMX) ... % temporary matrix
539 * twopi * fOpr; % (equivalent phase)
540 excPhsErr = excPhsErr + err (my + 1, mx + 1); % subarray-level error
541 err = (ofsTimeL + stdTimeL * randn (numLY, numLX)) * twopi * fOpr;
542 excPhsErr = excPhsErr + err (ly + 1, lx + 1); % subaperture-level error
543 excPhs = excPhsErr + excPhsIdl; % actual (with error) phases
544 clear err excPhsErr;
545
546 % Assemble complex excitations
547 %
548 exc = excMag .* exp (-i * excPhs);
549 % clear excMag excPhs;
550
551 % Calculate the field pattern (array factor)
552 %
553 % Here the DFT is calculated and the result rearranged into the
554 % desired region of direction cosine space. The element factor is
555 % unity. Mutual coupling is ignored.
556 %
557 g = fft2 (exc, tx); % first element is zero frequency
558 g = g (tIndx); % rearrange
559 gSqr = real (conj (g) .* g); % squared magnitude
560 gMag = sqrt (gSqr); % magnitude
561 clear g;
562
563 % Determine actual beam direction by fitting the transform
564 %
565 % This first of two methods for calculating the beam pointing vector
566 % uses the information in the Fourier transform of the excitations.
567 % First we locate the element of g with the largest value. (If the
568 % maximum value of elements is obtained by more than one element,
569 % this code will use the one with the smallest column index and the
570 % smallest row index within that column. Later processing will
571 % determine whether the multiple maxima are all within the main
572 % beam.) To estimate the location of the maximum of the underlying
573 % continuous function, that element and its eight neighbors are
574 % fitted to the elliptic paraboloid [1]
575 %
576 % 1 2 1 2
577 % - U x + W x y + - V y + X x + Y y + Z = |g (x, y)|
578 % 2 2
579 %
580 % (in the direction cosine coordinate system) in a least-squares
581 % sense. We employ the technique of QR decomposition to find the
582 % least-squares solution. Define the solution vector
583 %
584 % T
585 % a = [U W V X Y Z]
586 %
587 % of length M = 6, the ordinate (column) vector b with elements
588 %
589 % b = |g (x, y)|
590 % i i i
591 %
592 % of length N = 9 (number of fitted points), and the design matrix A
593 % having rows
594 %
595 % 1 2 1 2
596 % A = [ - x x y - y x y 1 ],
597 % i,: 2 i i i 2 i i i
598 %
599 % where the (x[i], y[i]) are the coordinates of the points
600 % neighboring and including the maximum element. QR decomposition
601 % of A factorizes it as
602 %
603 % A = Q R ,
604 %
605 % where Q is unitary (Q' Q = eye) and R is upper triangular. (We
606 % use Matlab's economy size decomposition, for which Q is M-by-N and
607 % R is N-by-N.) The least-squares solution of
608 %
609 % A a = b
610 %
611 % is given by
612 %
613 % -1
614 % a = R Q' b .
615 %
616 % The error in the solution depends on the degree to which the
617 % values of |g| depart from parabolic form, which is indicated by
618 % the reduced chi-square
619 %
620 % 2 1 2
621 % chi = -- chi ,
622 % nu nu
623 %
624 % where nu = N - M is the number of degrees of freedom and
625 %

```

```

626 %      2
627 %      chi = (A a - b)' (A a - b) .
628 %
629 % The covariance matrix for the solution vector is normally given by
630 % the matrix inverse of the curvature matrix
631 %
632 %      alpha = A' A ,
633 %
634 % whose elements are the second partial derivatives of chi^2 with
635 % respect to the elements of the solution vector [2]:
636 %
637 %      1 d      d      2
638 %      alpha = - ---- ---- chi .
639 %      mn 2 d a[m] d a[n]
640 %
641 % To incorporate the degree of deviation from parabolic form, we
642 % scale the covariance matrix by the reduced chi-square, as
643 %
644 %      2      -1      2      -1
645 %      C = chi (A' A) = chi (R' R) .
646 %      poly      nu      nu
647 %
648 % This completes the least-squares procedure.
649 %
650 % Having obtained the coefficients of the best-fit polynomial, we
651 % locate its maximum. The coordinates (plx, ply) of the maximum
652 % solve
653 %
654 %      / U W \ / plx \ / X \ / 0 \
655 %      |   |   | + |   | = |   | ;
656 %      \ W V \ \ ply / \ Y / \ 0 /
657 %
658 % that is,
659 %
660 %      / plx \ 1 / V -W \ X \
661 %      |   | = - |   | ,
662 %      \ ply / D \ -W U / Y /
663 %
664 % where
665 %
666 %      2
667 %      D = W - U V
668 %
669 % is the discriminant of the polynomial (and the negative
670 % determinant of the matrix). If the maximum so found lies outside
671 % the interpolation region, the region is expanded by one sample in
672 % each direction and the least-squares fit is repeated. This loop
673 % continues until the interpolation region exceeds a certain size or
674 % a satisfactory maximum is found. Assuming a maximum has been
675 % found, the covariance matrix for plx and ply is calculated next.
676 % We first form the derivative matrix or Jacobian
677 %
678 %      d (plx, ply)
679 %      J = -----
680 %      p      d (a)
681 %
682 %      / d plx d plx d plx d plx d plx d plx \
683 %      | d U d W d V d X d Y d Z |
684 %      = | d ply d ply d ply d ply d ply d ply |
685 %      | d U d W d V d X d Y d Z |
686 %
687 % The plx derivatives are
688 %
689 %      d plx V X - W Y
690 %      ----- = ----- V
691 %      d U      D^2
692 %
693 %      d plx W^2 Y + U V Y - 2 W V Y
694 %      ----- = -----
695 %      d W      D^2
696 %
697 %      d plx W X - U Y
698 %      ----- = ----- W
699 %      d V      D^2
700 %
701 %      d plx V
702 %      ----- = -
703 %      d X      D
704 %
705 %      d plx W
706 %      ----- = - ,
707 %      d Y      D
708 %
709 % and the ply derivatives follow by exchanging U for V and X for Y
710 % everywhere. The covariance matrix for plx and ply is simply
711 %
712 %      T
713 %      C = J C J .
714 %      p      poly p
715 %
716 %
717 %

```

```

718 %
719 % If no satisfactory maximum was found by the above procedure, the
720 % location of the maximum of |g| is used. A covariance matrix is
721 % fabricated for which the area of the 2 sigma ellipse equals the
722 % area of four grid squares to indicate the uncertainty in the
723 % actual location of the maximum.
724 %
725 % [1] D. H. von Seggern, _CRC Standard Curves and Surfaces_. Boca
726 % Raton, FL: CRC, 1993.
727 %
728 % [2] P. R. Bevington and D. K. Robinson, _Data Reduction and Error
729 % Analysis for the Physical Sciences_, 2nd ed. New York, NY:
730 % McGraw-Hill, 1992, pp. 121-125.
731 %
732 [gSqrMaxAct, gSqrMaxRow] = max (gSqr .* visBool); % maximum values and their rows
733 [gSqrMaxAct, gSqrMaxCol] = max (gSqrMaxAct); % overall maximum and column
734 gSqrMaxRow = gSqrMaxRow (gSqrMaxCol); % corresponding row
735 intRad = 1; % interpolation radius
736 p1OK = 0;
737 while ~p1OK & intRad < 4
738     p1Nbrs = [-intRad : intRad];
739     plx = dirCosXmtx (gSqrMaxRow + p1Nbrs, gSqrMaxCol + p1Nbrs); % neighbors
740     ply = dirCosYmtx (gSqrMaxRow + p1Nbrs, gSqrMaxCol + p1Nbrs);
741     plz = gMag (gSqrMaxRow + p1Nbrs, gSqrMaxCol + p1Nbrs);
742     plx = plx (:);
743     ply = ply (:);
744     plz = plz (:);
745     pDesMtx = [plx.*plx/2 plx.*ply ply.*ply/2 ... % design matrix
746               plx ply ones(size(plx))];
747     [Q, R] = qr (pDesMtx, 0); % now pDesMtx = Q * R; Q' * Q = eye
748     pPoly = R \ (Q' * plz); % solves pDesMtx * pPoly = plz
749     dof = length (plz) - length (pPoly); % degrees of freedom in the fit
750     chiSqr = plz - pDesMtx * pPoly; % deviations only
751     chiSqr = chiSqr' * chiSqr; % now sum of squared deviations
752     pPolyVar = inv (R' * R) * chiSqr / dof; % pDesMtx' * pDesMtx = R' * R
753     pVec = [-pPoly(1) pPoly(2); pPoly(2) pPoly(3)] ... % find critical point
754             \ [pPoly(4); pPoly(5)];
755     p1OK = ... % is interpolated point
756             (pVec (1) > dirCosX (gSqrMaxCol - intRad)) ... % inside neighborhood?
757             & (pVec (1) < dirCosX (gSqrMaxCol + intRad)) ... % (pathological cases can
758             & (pVec (2) > dirCosY (gSqrMaxRow - intRad)) ... % place it outside)
759             & (pVec (2) < dirCosY (gSqrMaxRow + intRad));
760     if ~p1OK
761         intRad = intRad + 1;
762     end
763 end
764 if p1OK
765     plx = pVec (1); % keep interpolated point
766     ply = pVec (2);
767     pDet = pPoly (2)^2 - pPoly (1) * pPoly (3); % determinant
768     plxDer = [(1 -1)*(pPoly([3 2])).*pPoly([4 5]))*pPoly(3)/pDet
769              (1 1 -2)*(pPoly([2 1 2])).*pPoly([2 3 3])).*pPoly([5 5 4]))/pDet
770              (1 -1)*(pPoly([2 1])).*pPoly([4 5]))*pPoly(2)/pDet
771              pPoly(3)
772              -pPoly(2)
773              0 ]' / pDet; % derivatives
774     plyDer = [(1 -1)*(pPoly([2 3])).*pPoly([5 4]))*pPoly(2)/pDet
775              (1 1 -2)*(pPoly([2 3 2])).*pPoly([2 1 1])).*pPoly([4 4 5]))/pDet
776              (1 -1)*(pPoly([1 2])).*pPoly([5 4]))*pPoly(1)/pDet
777              -pPoly(2)
778              pPoly(1)
779              0 ]' / pDet;
780     plVar = [plxDer; plyDer] * pPolyVar * [plxDer; plyDer]'; % covariance matrix
781 else
782     plx = dirCosXmtx (gSqrMaxRow, gSqrMaxCol); % use location of
783     ply = dirCosYmtx (gSqrMaxRow, gSqrMaxCol); % actual maximum
784     plVar = diag (1 ./ (pi * [txLim tyLim]^2)); % 2 sigma area = 4 grid squares
785 end
786 clear intRad p1OK p1Nbrs plz pDesMtx Q R pPoly;
787 clear dof chiSqr pPolyVar pVec pDet plxDer plyDer;
788
789 % Determine actual beam direction by fitting the excitation phases
790 %
791 % The second method for calculating the pointing vector uses the
792 % excitation magnitudes and phases, not the transform. For brevity,
793 % define
794 %
795 % Delta (x, y) = k n dx x + k m dy y + theta ,
796 % mn mn
797 %
798 % where the theta[m,n] are the excitation phases, and let e[m,n]
799 % denote the excitation magnitudes. When we express the power
800 % pattern as
801 %
802 %
803 % |g (x, y)| = sum sum sum sum e e
804 % m1 n1 m2 n2 m1,n1 m2,n2
805 %
806 % * exp [i (Delta - Delta )]
807 % m1,n1 m2,n2
808 %

```

```

809      %
810      % 
$$= \sum_{m,n} e^{2} + 2 \sum_{m_1,n_1} \sum_{m_2,n_2} e^{m_1,n_1} e^{m_2,n_2}$$

811      %
812      %
813      % 
$$+ \cos(\Delta_{m_1,n_1} - \Delta_{m_2,n_2})$$

814      %
815      %
816      % where the primed sum is over distinct pairs (m1, n1) and (m2, n2),
817      % we see that the maximum occurs where the cosine contributions are
818      % largest. If the phase front is nearly flat, the arguments of the
819      % cosines will be small for (x, y) near the direction of phase front
820      % propagation. To fourth order in the arguments,
821      %
822      % 
$$|g(x, y)|^2 = \left( \sum_{m,n} e^{2} + 2 \sum_{m_1,n_1} \sum_{m_2,n_2} e^{m_1,n_1} e^{m_2,n_2} \right)$$

823      %
824      %
825      % 
$$\frac{1}{2} \left( \Delta_{m_1,n_1}^2 - \Delta_{m_2,n_2}^2 \right)$$

826      %
827      %
828      % 
$$+ \frac{1}{24} \left( \Delta_{m_1,n_1}^4 - \Delta_{m_2,n_2}^4 \right)$$

829      %
830      %
831      %
832      %
833      %
834      % Keeping terms to only second order, we are motivated to find the x
835      % and y (implicit in Delta[mn]) that minimize
836      %
837      % 
$$\chi^2 = \sum_{m_1,n_1} \sum_{m_2,n_2} e^{m_1,n_1} e^{m_2,n_2} (\Delta_{m_1,n_1}^2 - \Delta_{m_2,n_2}^2)^2$$

838      %
839      %
840      %
841      % where the subscript 2 denotes the second-order truncation. Taking
842      % derivatives with respect to x and y and rearranging yields the
843      % normal equations
844      %
845      % 
$$\frac{\partial}{\partial x} \left( \sum_{m_1,n_1} \sum_{m_2,n_2} e^{m_1,n_1} e^{m_2,n_2} \frac{\partial}{\partial x} (\Delta_{m_1,n_1}^2 - \Delta_{m_2,n_2}^2) \right) = 0$$

846      %
847      %
848      %
849      % 
$$+ \frac{\partial}{\partial x} \left( [n_1 - n_2] \Pi + \theta_{m_1,n_1} - \theta_{m_2,n_2} \right) = 0$$

850      %
851      %
852      %
853      % where  $\Pi = k [dx^2 + dy^2]$ . Here the sums contain a total of
854      % (numLMNX*2 numLMNY*2) terms, which may be of the order of one
855      % million for a typical array. To reduce this number, we transform
856      % the least-squares problem to an equivalent but simpler problem.
857      % First, the above normal equations may be rewritten with the column
858      % vector  $[n_1 - n_2]'$  replaced by  $[n_1 \ m_1]'$ , which may be seen by
859      % separating the column vector into two sums and exchanging (m1,n1)
860      % with (m2,n2) in one of the sums. Second, the row vector may be
861      % separated into two sums to obtain
862      %
863      % 
$$\frac{\partial}{\partial x} \left( \sum_{m,n} e^{m,n} \frac{\partial}{\partial x} (\sum_{m,n} e^{m,n} [n \ m] \Pi + \theta_{m,n}) \right) = 0$$

864      %
865      %
866      %
867      % 
$$- \sum_{m,n} e^{m,n} \frac{\partial}{\partial x} \left( \sum_{m,n} e^{m,n} ([n \ m] \Pi + \theta_{m,n}) \right) = 0$$

868      %
869      %
870      %
871      % Based on the second term, we define
872      %
873      % 
$$\Delta = \frac{\sum_{m,n} e^{m,n} ([n \ m] \Pi + \theta_{m,n})}{\sum_{m,n} e^{m,n}}$$

874      %
875      %
876      %
877      %
878      %
879      % Finally, we may rewrite the normal equations as
880      %
881      % 
$$\frac{\partial}{\partial x} \left( \sum_{m,n} e^{m,n} \frac{\partial}{\partial x} ([n \ m] \Gamma + \theta_{m,n}) \right) = 0$$

882      %
883      %
884      %
885      % where  $\Gamma = [k^2 dx^2 + k^2 dy^2 \Delta]$  and the third row follows
886      % from the definition of Delta. These normal equations contain only
887      % (numLMNX numLMNY) terms, nominally on the order of 1000. They
888      % find the plane  $k n dx + k m dy + \Delta$  that best fits
889      %  $-\theta_{m,n}$  in a weighted least-squares sense. The solution is
890      % found using QR decomposition of the design matrix, which has rows
891      %  $[n \ m \ 1]$ .
892      %
893      % The error in the solution is determined not by the deviations of
894      % the  $-\theta_{m,n}$  from the best-fit plane nor by the deviations
895      %  $\Delta_{m_1,n_1} - \Delta_{m_2,n_2}$  appearing in  $\chi^2$  earlier, for the
896      % solution is exactly the power pattern maximum to second order in
897      % the cosine arguments. However, the error does depend on the
898      % fourth and higher powers of the cosine arguments. So motivated,
899      % we consider the fourth-order merit function
900      %

```

```

901 %      2
902 %      chi = sum sum e e (Delta - Delta )
903 %      4 m1,n1 m2,n2 m1,n1 m2,n2 m1,n1 m2,n2
904 %
905 %      / 1 2 \
906 %      * | 1 - -- (Delta - Delta ) |
907 %      \ 12 m1,n1 m2,n2 /
908 %
909 % and observe that chi4^2 =< chi2^2 everywhere. We interpret the
910 % difference chi2^2 - chi4^2 as indicative of the error in the
911 % solution, and we scale the covariance matrix by that amount. The
912 % covariance matrix used is the inverse of the curvature matrix for
913 % chi2^2; that curvature matrix is
914 %
915 %      2
916 %      alpha = k sum sum e e
917 %      m1,n1 m2,n2 m1,n1 m2,n2
918 %
919 %      / (n1-n2)dx \
920 %      * | 1 - -- (n1-n2)dx (m1-m2)dy | .
921 %      \ (m1-m2)dy /
922 %
923 % Because we construct the design matrix for the simpler
924 % least-squares problem, we must construct alpha explicitly.
925 % However, this can be accomplished by analytically expanding the
926 % differences and factoring the sums.
927 %
928 pbsX = ones (numLMNY, 1) * nx * dx * (twopi * fOpr / c);
929 pbsY = ny * ones (1, numLMNX) * dy * (twopi * fOpr / c);
930 pbsX = pbsX (:);
931 pbsY = pbsY (:);
932 excMagV = excMag (:);
933 desMtx = [pbsX pbsY ones(numLMNX*numLMNY,1)] ...
934 .* (sqrt (excMagV) * ones (1, 3));
935 [Q, R] = qr (desMtx, 0); % now desMtx = Q * R and Q' * Q = eye [conj. transpose]
936 excPbsWgt = -excPbs (:). * sqrt (excMagV);
937 p2Vec = R \ (Q' * excPbsWgt); % desMtx * p2Vec = excPbsWgt
938 p2x = p2Vec (1);
939 p2y = p2Vec (2);
940 DeltaPbs = [pbsX pbsY ones(numLMNX*numLMNY,1)] * p2Vec + excPbs (:);
941 sumExcMagDelta1 = excMagV .* DeltaPbs;
942 sumExcMagDelta2 = sumExcMagDelta1 .* DeltaPbs;
943 sumExcMagDelta3 = sumExcMagDelta2 .* DeltaPbs;
944 sumExcMagDelta4 = sumExcMagDelta3 .* DeltaPbs;
945 sumExcMagDelta0 = sum (excMagV);
946 sumExcMagDelta1 = sum (sumExcMagDelta1);
947 sumExcMagDelta2 = sum (sumExcMagDelta2);
948 sumExcMagDelta3 = sum (sumExcMagDelta3);
949 sumExcMagDelta4 = sum (sumExcMagDelta4);
950 chiSqrRed = ( 2 * sumExcMagDelta4 + sumExcMagDelta0 ...
951 - 8 * sumExcMagDelta3 + sumExcMagDelta1 ...
952 + 6 * sumExcMagDelta2 + sumExcMagDelta2 ) / 12;
953 chiSqrRed = max (0, chiSqrRed); % in case of roundoff error
954 excMagPbs = excMagV * [pbsX pbsY];
955 crvMtx = 2 * sumExcMagDelta0 * [pbsX pbsY]' ...
956 * ([pbsX pbsY] .* [excMagV excMagV]) ...
957 - 2 * excMagPbs' * excMagPbs;
958 p2Var = chiSqrRed * inv (crvMtx);
959 clear pbsX pbsY excMagV desMtx Q R excPbsWgt p2Vec DeltaPbs;
960 clear sumExcMagDelta0 sumExcMagDelta1 sumExcMagDelta2 sumExcMagDelta3 sumExcMagDelta4;
961 clear chiSqrRed excMagPbs crvMtx;
962
963 % Construct pointing vector
964 %
965 % Above we constructed two pointing vectors by different methods.
966 % The method of fitting the transform is robust even for large
967 % errors but limited by the transform resolution. On the other
968 % hand, the method of fitting the excitation phases is independent
969 % of transform resolution but accurate only for small errors,
970 % approaching the exact solution as the phase errors decrease. We
971 % wish to obtain a single pointing vector for subsequent use, and
972 % for this purpose we form a weighted average. Specifically, each
973 % vector is weighted by the inverse of the area of its covariance
974 % ellipse, which is pi times the determinant of the covariance
975 % matrix. Similarly, a single covariance matrix is obtained by
976 % weighing each covariance matrix by the square of the pointing
977 % vector weights, normalized to avoid effectively halving the
978 % covariance matrix when the two incoming matrices are nearly equal.
979 %
980 area1 = det (p1Var);
981 area2 = det (p2Var);
982 areaTot = area1 + area2;
983 wght1 = area2 / areaTot;
984 wght2 = area1 / areaTot;
985 px = wght1 * p1x + wght2 * p2x;
986 py = wght1 * p1y + wght2 * p2y;
987 pVar = (wght1^2 * p1Var + wght2^2 * p2Var) / (wght1^2 + wght2^2);
988 clear area1 area2 areaTot wght1 wght2;
989 clear p1x p1y p1Var;
990 clear p2x p2y p2Var;
991
992 % Calculate peak power density and pointing error

```



```

993 %
994 % To avoid inaccuracies due to interpolation, the peak power
995 % density is obtained by explicitly evaluating the Fourier
996 % transform at the pointing vector. The pointing error is
997 % straightforwardly calculated from the dot product of the steering
998 % and pointing vectors. However, an optional second method is
999 % coded that makes use of the pointing vector covariance matrix to
1000 % calculate the uncertainty (standard deviation) of the pointing
1001 % error due to uncertainty in the pointing vector. If this
1002 % uncertainty is desired, also uncomment lines elsewhere that refer
1003 % to errPointUnc and errPointUncS.
1004 %
1005 pxy2 = px^2 + py^2;
1006 peakVisb = (pxy2 <= 1);
1007 if peakVisb
1008     gSqrMax = exp (-i * twopi * (fOpr / c) ... % complex field
1009     * ( px * dx * ones (numLMNY, 1) * nx ...
1010     + py * dy * ny * ones (1, numLMNX))) .* exc;
1011     gSqrMax = sum (gSqrMax ()); % phaser sum
1012     gSqrMax = real (conj (gSqrMax) * gSqrMax); % power
1013     pz = sqrt (1 - pxy2);
1014     if 0 % INPUT 0 to skip std dev, 1 to calc
1015         pCrs = [ 0 -sz sy % cross product
1016                 sz 0 -sx
1017                 -sy sx 0 ] * [px py pz]';
1018         pCrsDer = [ -sy*px/pz -sz-sy*py/pz % rows correspond to
1019                    sz+sx*px/pz sx*py/pz % components of pCrs;
1020                    -sy sx ]'; % columns, to pVec
1021         pCrsVar = pCrsDer * pVar * pCrsDer'; % covariance matrix
1022         pCrsMag = sqrt (pCrs' * pCrs); % magnitude
1023         if pCrsMag > 0
1024             pCrsMagDer = pCrs' / pCrsMag; % derivative exists
1025             pCrsMagVar = pCrsMagDer * pCrsVar * pCrsMagDer';
1026         else % derivative doesn't exist
1027             pCrsMagVar = trace (pCrsVar) / 3; % average of principal variances
1028         end
1029         errPoint = asin (pCrsMag);
1030         errPointUnc = abs (1 / sqrt (1 - pCrsMag^2)) * sqrt (pCrsMagVar);
1031         clear pCrs pCrsDer pCrsVar pCrsMag pCrsMagDer pCrsMagVar;
1032     else
1033         errPoint = acos (min (1, ... % dot product for error; min
1034                             sx * px + sy * py + sz * pz)); % prevents roundoff problems
1035         errPointUnc = nan;
1036     end
1037 else % maximum is invisible
1038     gSqrMax = gSqrMaxAct;
1039     px = nan;
1040     py = nan;
1041     pz = nan;
1042     errPoint = nan;
1043     errPointUnc = nan;
1044 end
1045 beamPowerDB = 10 * log10 (gSqrMax);
1046 clear pxy2;
1047
1048 % Determine main beam region
1049 %
1050 % The angular domain of the main beam is constructed starting with
1051 % the maximum element. The largest neighboring element is added on,
1052 % followed by the largest neighbor of either point, and so on. This
1053 % accretion continues until any neighbor of the largest element on
1054 % the main beam border exceeds the element added previously.
1055 % Effectively, elements are added with values descending from the
1056 % peak until an opportunity to ascend is reached. All visible
1057 % elements outside of the main beam are declared to be in the
1058 % sidelobes.
1059 %
1060 beamWidLvl = gSqrMax / 2; % power level where beam width is measured
1061 adjc = [-ay-1 -ay -ay+1 -1 1 ay-1 ay ay+1]; % relative indices of neighbors
1062 % Note: We must include the diagonal neighbors in order to
1063 % correctly descend a structure such as [1 0.4; 0.5 0.9].
1064 beamBool = logical (zeros (ay, ax)); % build main beam in Boolean variable
1065 brdrLen = 1;
1066 brdrIndx = (gSqrMaxCol - 1) * ay + gSqrMaxRow; % start with maximum
1067 brdrVal = 0; % any value will do here
1068 beamBool (brdrIndx) = 1; % main beam begins with maximum
1069 adjcIndx = brdrIndx + adjc'; % and neighbors
1070 adjcIndx = adjcIndx (visBool (adjcIndx)); % that are visible
1071 adjcVal = gSqr (adjcIndx); % get values
1072 beamDepth = inf; % get the loop started
1073 beamVisb = 1;
1074 capVisb = (gSqrMaxAct > beamWidLvl); % usually true unless resolution is too low
1075 while max (adjcVal) <= beamDepth % are the new neighbors all downhill?
1076     brdrLen = brdrLen + 1; % yes; remove element from border
1077     brdrIndx = brdrIndx (1 : brdrLen);
1078     brdrVal = brdrVal (1 : brdrLen);
1079     beamBool (adjcIndx) = ones (size (adjcIndx)); % add neighbors to main beam
1080     for adjcPtr = 1 : length (adjcIndx) % and to border
1081         pos = sum (brdrVal <= adjcVal (adjcPtr)); % ordered least to greatest
1082         brdrIndx = [brdrIndx(1:pos) adjcIndx(adjcPtr) brdrIndx(pos+1:brdrLen)];
1083         brdrVal = [brdrVal(1:pos) adjcVal(adjcPtr) brdrVal(pos+1:brdrLen)];
1084     end
1085     brdrLen = brdrLen + 1;

```

```

1085     end
1086     beamDepth = brdrVal (brdrLen); % pick largest element from border
1087     adjcIndx = brdrIndx (brdrLen) + adjc; % neighbors of chosen element
1088     adjcIndx = adjcIndx (visBool (adjcIndx)); % eliminate invisible points
1089     if length (adjcIndx) < length (adjc) % were some invisible?
1090         beamVisb = 0; % yes; clear flag
1091         if beamDepth >= beamWidLvl % are we below the threshold?
1092             capVisb = 0; % no; the cap is partially invisible
1093     end
1094     end
1095     adjcIndx = adjcIndx (~beamBool (adjcIndx)); % use only new elements
1096     adjcVal = gSqr (adjcIndx); % and get their values
1097 end
1098 capClosed = capVisb & (beamDepth < beamWidLvl); % closed contour at beamWidLvl?
1099 sideBool = visBool & ~beamBool; % sidelobe region
1100 beamIndx = find (beamBool);
1101 if max (max (gSqr (sideBool))) < gSqrMaxAct % duplicate maximum outside beam?
1102     beamExist = 1; % no; the beam is identified
1103     if ~peakVisb
1104         disp ('Warning: The main beam peak is invisible; some calculations');
1105         disp (' may return NaN.');
```

$$-Ux^2 + Wxy + \frac{1}{2}Vy^2 + Xx + Yy + Z = 0$$

```

1157     %
1158     %
1159     % using a simple algorithm that minimizes the algebraic distance as
1160     % follows. Define the design matrix D to have rows
1161     %
1162     %      1 2      1 2
1163     %      D = [ (- x ) (x y) (- y ) x y 1],
1164     %      i,:  2 i   i i  2 i   i i
1165     %
1166     % where the (x[i], y[i]) are the points along the contour, and let the
1167     % coefficient vector be
1168     %
1169     %      a = [U W V X Y Z] .
1170     %
1171     %
1172     % The algebraic distance between a point and a conic section is the
1173     % left-hand side of the conic section equation, so that the distance
1174     % between a point i along the contour and the ellipse described by the
1175     % vector a is simply D[i,:]*a. We seek the minimum of the sum of
1176     % squared algebraic distances, which is just ||D a||^2, subject to the

```

```

1177 % constraint ||a||^2 = 1. We therefore introduce the constrained
1178 % objective function
1179 %
1180 %
1181 %  $E = ||D a||^2 - \lambda (||a||^2 - 1)$ 
1182 %
1183 %  $T \quad T \quad T$ 
1184 %  $= a^T D D a - \lambda (a^T a - 1)$ 
1185 %
1186 % where lambda is a Lagrange multiplier. The minimum is found
1187 % analytically to occur when
1188 %
1189 %  $D D a = \lambda a$ ,
1190 %
1191 %
1192 % which is an eigenvalue equation. The desired coefficient vector, a,
1193 % corresponds to the minimum eigenvalue.
1194 %
1195 % Using the coefficients of the best-fit ellipse, we now calculate
1196 % the beam characteristics. First, a sign change is applied to the
1197 % coefficients if necessary to force U (and therefore V) to be
1198 % negative. For convenience, we rewrite the conic section as
1199 %
1200 %  $\frac{1}{2} p^T A p + B^T p + Z = 0$ ,
1201 %
1202 %
1203 %
1204 % where p = [x; y],
1205 %
1206 %  $A = \begin{bmatrix} U & W \\ W & V \end{bmatrix}$ ,
1207 %
1208 %
1209 % and B = [X; Y]. We first find the center of the ellipse in order
1210 % to draw it later. Replacing p with p + p1 in the conic section
1211 % yields
1212 %
1213 %
1214 %  $\frac{1}{2} p1^T A p1 + (p^T A + B)^T p1 + Z1 = 0$ ,
1215 %
1216 %
1217 %
1218 % where
1219 %
1220 %  $Z1 = -\frac{1}{2} p^T A p + B^T p + Z$ 
1221 %
1222 %
1223 % is defined for later use. When p coincides with the center, the
1224 % linear term vanishes; therefore, p solves
1225 %
1226 %  $A p + b = 0$ .
1227 %
1228 %
1229 % We next find the roll angle, which is conceptually defined as
1230 % follows, using spherical, not stereographic, coordinates. If the
1231 % ellipse center is not at boresight, rotate it (and the antenna
1232 % pattern) to boresight along the great circle connecting the two.
1233 % The angle from the great circle with azimuth 0 to the great circle
1234 % along the beam's major axis (direction of maximum width) is the
1235 % roll angle. Alternatively, construct the great circle connecting
1236 % the ellipse center and boresight. The roll angle is the sum of
1237 % two angles, the angle from the great circle with azimuth 0 to the
1238 % constructed great circle and the angle from the constructed great
1239 % circle to the great circle along the beam's major axis. Now the
1240 % roll angle so defined is merely the apparent orientation of the
1241 % major axis when viewed in the stereographic projection. In a
1242 % (stereographic) coordinate system rotated by that angle, the
1243 % off-diagonal element of A (the coefficient W) vanishes; therefore,
1244 % we seek the coordinate system that diagonalizes A. Replacing p
1245 % with R p2 in the original conic section gives
1246 %
1247 %  $\frac{1}{2} p2^T (R^T A R) p2 + (B^T R) p2 + Z = 0$ .
1248 %
1249 %
1250 %
1251 % The new quadratic coefficient R^T A R will be diagonal if the
1252 % columns of R are the eigenvectors of A. The new diagonal elements
1253 % U2 and V2 become the eigenvalues, which are explicitly
1254 %
1255 %  $U2 = \frac{U+V}{2} + \frac{\sqrt{(U-V)^2 + 4W^2}}{2}$  and
1256 %
1257 %  $V2 = \frac{U+V}{2} - \frac{\sqrt{(U-V)^2 + 4W^2}}{2}$ .
1258 %
1259 %
1260 %
1261 %
1262 %
1263 % The eigenvalue with the smaller magnitude (U2 above, since U and V
1264 % are negative) corresponds to the major axis. Therefore, the
1265 % corresponding eigenvector points along the direction of the major
1266 % axis; the other eigenvector, along the minor axis. The roll angle
1267 % is obtained from the two components of the major axis; explicitly,
1268 % it satisfies

```

```

1269 %
1270 %
1271 %      2 W
1272 %      tan (2 roll) = -----
1273 %      U - V
1274 %
1275 % We also use the eigenvectors to draw the ellipse later. Last, the
1276 % eigenvalues yield the major and minor full widths at half maximum
1277 % of the main beam as
1278 %
1279 %      /   Z1 \1/2      /   Z1 \1/2
1280 %      | -8 -- |      and | -8 -- | ,
1281 %      \   U2 /      \   V2 /
1282 %
1283 % respectively. As these were derived in the stereographic
1284 % projection, a factor of (1 + cos polar) is applied to obtain the
1285 % approximate widths in real angles.
1286 %
1287 if capClosed
1288 %
1289 % Construct the contour
1290 %
1291 capIndx = beamIndx (gSqr (beamIndx) >= beamWidLvl); % elements at or above level
1292 capBool = logical (zeros (ay, ax));
1293 capBool (capIndx) = ones (size (capIndx));
1294 adjc = [ay ay+1 1 -ay+1 -ay -ay-1 -1 ay-1]; % clockwise in matrix row-column coordinates
1295 dirIndx = 1; % initial index into adjc
1296 intIndx = capIndx (1); % initial index of interpolation center
1297 dirIndxSt = 0; % get loop started
1298 intIndxSt = 0;
1299 capContX = []; % empty contour coordinates
1300 capContY = [];
1301 while capBool (intIndx + adjc (dirIndx)) % next element is inside cap?
1302     intIndx = intIndx + adjc (dirIndx); % keep moving until edge is reached
1303 end
1304 while (intIndx ~= intIndxSt) | (dirIndx ~= dirIndxSt) % back at starting point?
1305     adjcInc = abs (adjc (dirIndx)); % no; get magnitude
1306     if (adjcInc == 1) | (adjcInc == ay) % looking across row or column?
1307         if adjcInc == ay % across column?
1308             capContY1 = dirCosYmtx (intIndx); % yes; interpolate in x
1309             capContX1 = dirCosXmtx (intIndx) + (beamWidLvl - gSqr (intIndx)) ...
1310                 * (dirCosXmtx (intIndx + adjc (dirIndx)) - dirCosXmtx (intIndx)) ...
1311                 / (gSqr (intIndx + adjc (dirIndx)) - gSqr (intIndx));
1312         else % across row
1313             capContX1 = dirCosXmtx (intIndx); % interpolate in y
1314             capContY1 = dirCosYmtx (intIndx) + (beamWidLvl - gSqr (intIndx)) ...
1315                 * (dirCosYmtx (intIndx + adjc (dirIndx)) - dirCosYmtx (intIndx)) ...
1316                 / (gSqr (intIndx + adjc (dirIndx)) - gSqr (intIndx));
1317         end
1318         if isempty (capContX) % first point?
1319             capContX = capContX1; % yes; store it
1320             capContY = capContY1;
1321             intIndxSt = intIndx; % remember starting point
1322             dirIndxSt = dirIndx;
1323         elseif (capContX (length (capContX)) ~= capContX1) ... % duplicate? (e.g.,
1324             & (capContY (length (capContY)) ~= capContY1) % element equals level)
1325             capContX = [capContX; capContX1]; % no; append it
1326             capContY = [capContY; capContY1];
1327         end
1328     end
1329     dirIndx = dirIndx + 1; % (no diagonal interpolation)
1330     if dirIndx > length (adjc) % next direction
1331         dirIndx = 1; % cycle
1332     end
1333     adjcInc = abs (adjc (dirIndx)); % no; get magnitude of step
1334     if capBool (intIndx + adjc (dirIndx)) % next element is inside cap?
1335         intIndx = intIndx + adjc (dirIndx); % yes; becomes new interpolation center
1336         dirIndx = dirIndx - length (adjc) / 2 + 1; % reverse, then ahead one increment
1337         if (adjcInc == 1) | (adjcInc == ay) % stepped in row or column?
1338             dirIndx = dirIndx + 1; % yes; ahead an extra increment
1339             % (useless to look back diagonally)
1340         end
1341         if dirIndx < 1 % cycle
1342             dirIndx = dirIndx + length (adjc);
1343         end
1344     end
1345 end % while % contour complete
1346 %
1347 % Fit an ellipse in stereographic coordinates
1348 %
1349 capContZ = sqrt (1 - capContX.^2 - capContY.^2);
1350 capContXS = capContX ./ (1 + capContZ); % to stereographic coords
1351 capContYS = capContY ./ (1 + capContZ);
1352 cDesMtx = [capContXS.*capContXS/2 capContXS.*capContYS ... % to form design matrix
1353             capContYS.*capContYS/2 capContXS ... % for least-squares fit
1354             capContYS ones (size (capContXS))];
1355 cDesMtx = cDesMtx' * cDesMtx; % done
1356 capContX = capContX ([1:length (capContX) 1]); % close contour for plotting
1357 capContY = capContY ([1:length (capContY) 1]);
1358 capContZ = capContZ ([1:length (capContZ) 1]);
1359 [cEigVec, cEigVal] = eig (cDesMtx); % eigenvectors and -values
1360 [cEigValMin, cEigValMinIdx] = min (diag (cEigVal)); % minimum eigenvalue
1361 cPoly = cEigVec (:, cEigValMinIdx); % and matching vector
1362 cPoly = -cPoly * sign (cPoly (1)); % to have negative eigenvalues below

```

```

1361 %
1362 % Obtain beam characteristics from ellipse coefficients
1363 %
1364 cHessMtx = [cPoly(1) cPoly(2) % Hessian matrix;
1365             cPoly(2) cPoly(3)]; % second derivatives
1366 cDervMtx = [cPoly(4) % first derivative matrix
1367             cPoly(5)];
1368 capCenter = -cHessMtx \ cDervMtx; % ellipse center
1369 capConst = cPoly(6) + cDervMtx' * capCenter / 2; % new constant coefficient
1370 [cEigVec, cEigVal] = eig(cHessMtx);
1371 [cEigVal, cEigValOrd] = sort(diag(cEigVal)); % ascending order
1372 cEigVec = cEigVec(:, cEigValOrd); % corresponding order
1373 if cEigVec(1, 2) == 0 % special case?
1374     roll = pi / 2;
1375 else
1376     roll = atan(cEigVec(2, 2) / cEigVec(1, 2)); % angle to major axis
1377 end
1378 roll = roll - pi/2 + azmthOffst; % make -pi/2 <
1379 roll = roll - ceil(roll / pi) * pi + pi/2 - azmthOffst; % roll + azmthOffst <= pi/2
1380 hpbw = sqrt(-8 * capConst ./ cEigVal); % two-vector
1381 %
1382 % Construct the fitted ellipse for plotting (in stereographic coordinates)
1383 %
1384 theta = (0 : 10 / 360 : 1) * twopi;
1385 cFit = capCenter + ones(size(theta)) ... % calculate some
1386       + 0.5 * (cEigVec * diag(hpbw) ... % points along the
1387              * [sin(theta); cos(theta)]); % fitted ellipse
1388 cFitR2 = sum(cFit.^2); % squared radius in stereographic coords
1389 cFitZ = (1 - cFitR2) ./ (1 + cFitR2); % z direction cosine
1390 cFitX = cFit(1, :) .* (1 + cFitZ); % undo stereographic projection
1391 cFitY = cFit(2, :) .* (1 + cFitZ);
1392 hpbw = hpbw * (1 + pz); % undo widths, too
1393 hpbwMjr = hpbw(2);
1394 hpbwMnr = hpbw(1);
1395 else
1396     roll = nan;
1397     hpbwMjr = nan;
1398     hpbwMnr = nan;
1399 end
1400 clear capBool adjc dirIndx intIndx dirIndxSt intIndxSt adjcInc capContXl capContYl;
1401 clear capContXS capContYS cDesMtx cEigVec cEigVal cEigValMin cEigValMinIdx cPoly;
1402 clear cHessMtx cDervMtx capCenter capConst cEigValOrd hpbw;
1403 clear theta cFit cFitR2;
1404
1405 % Calculate power in visible space, main beam, and sidelobes; main
1406 % beam and sidelobe solid angles; and average sidelobe level
1407 %
1408 % These calculations involve integrals over the hemisphere or portions
1409 % of it. The integrals are carried out in direction cosine
1410 % coordinates by multiplying the integrand by the appropriate
1411 % Jacobian.
1412 %
1413 % The integrals are evaluated using the midpoint approximation, for
1414 % which the starting point is the Taylor series expansion of g(x, y)
1415 % to second order:
1416 %
1417 % 
$$g(a + u, b + v) = \frac{1}{2} \left[ g(a, b) + u \frac{\partial g}{\partial x} + v \frac{\partial g}{\partial y} + \frac{1}{2} \left( u^2 \frac{\partial^2 g}{\partial x^2} + 2uv \frac{\partial^2 g}{\partial x \partial y} + v^2 \frac{\partial^2 g}{\partial y^2} \right) \right]$$

1418 %
1419 %
1420 %
1421 %
1422 %
1423 % Then
1424 %
1425 % 
$$\frac{1}{2} \left[ \frac{c}{d} \frac{d}{d^2} \frac{\partial}{\partial u} \frac{\partial}{\partial v} g(a + u, b + v) = \frac{1}{24} \left[ c \frac{d}{d^2} \frac{\partial}{\partial x} \frac{\partial}{\partial y} g(a, b) + d \frac{\partial}{\partial x} \frac{\partial}{\partial y} g(a, b) \right] \right]$$

1426 %
1427 %
1428 %
1429 %
1430 %
1431 %
1432 %
1433 % The midpoint approximation keeps the first term and neglects the
1434 % quadratic terms. The maximum amount neglected is
1435 %
1436 % 
$$\frac{c}{24} \left[ \frac{d}{d^2} \frac{\partial}{\partial x} \frac{\partial}{\partial y} g(a, b) + d \frac{\partial}{\partial x} \frac{\partial}{\partial y} g(a, b) \right]$$

1437 %
1438 %
1439 %
1440 % which we use as the error estimate for each interior point of the
1441 % integration, approximating the second derivatives with scaled second
1442 % differences.
1443 %
1444 % To the interior error is added an estimate of the error due to
1445 % finite sampling at the integral limits; the estimate is half the
1446 % value of the integrand at the outermost samples.
1447 %
1448 % (The error estimate calculations have been commented out for
1449 % speed.)
1450 %
1451 % visbEdgeIndx = visBool;
1452 % visbEdgeIndx(2 : ay - 1, 2 : ax - 1) = ...

```

```

1453 % ( visbEdgeIdx (2 : ay - 1, 3 : ax) & visbEdgeIdx (1 : ay - 2, 2 : ax - 1) ...
1454 % & visbEdgeIdx (2 : ay - 1, 1 : ax - 2) & visbEdgeIdx (3 : ay , 2 : ax - 1) );
1455 % visbEdgeIdx = find (visbBool - visbEdgeIdx);
1456 % beamEdgeIdx = zeros (ay, ax);
1457 % beamEdgeIdx (beamIdx) = ones (size (beamIdx));
1458 % sideEdgeIdx = beamEdgeIdx;
1459 % beamEdgeIdx (2 : ay - 1, 2 : ax - 1) = ...
1460 % ( beamEdgeIdx (2 : ay - 1, 3 : ax) & beamEdgeIdx (1 : ay - 2, 2 : ax - 1) ...
1461 % & beamEdgeIdx (2 : ay - 1, 1 : ax - 2) & beamEdgeIdx (3 : ay , 2 : ax - 1) );
1462 % beamEdgeIdx (beamIdx) = 1 - beamEdgeIdx (beamIdx);
1463 % beamEdgeIdx = find (beamEdgeIdx);
1464 % sideEdgeIdx (2 : ay - 1, 2 : ax - 1) = ...
1465 % ( sideEdgeIdx (2 : ay - 1, 3 : ax) | sideEdgeIdx (1 : ay - 2, 2 : ax - 1) ...
1466 % | sideEdgeIdx (2 : ay - 1, 1 : ax - 2) | sideEdgeIdx (3 : ay , 2 : ax - 1) );
1467 % sideEdgeIdx (beamIdx) = zeros (size (beamIdx));
1468 % sideEdgeIdx = find (sideEdgeIdx);
1469 areaFact = zeros (ay, ax); % areal factor for integrating:
1470 areaFact = ... % Jacobian [1 / cos polar]
1471 1 ./ (txLim * tyLim * dirCosZmtx (visbBool)); % and grid spacing
1472 areaFactLim = 2 / sqrt (txLim * tyLim); % edge points may exceed this
1473 tooBig = find (areaFact > areaFactLim); % arbitrary limit; force those
1474 areaFact (tooBig) = ones (size (tooBig)) * areaFactLim; % that do to comply
1475 % sldAng = sum (areaFact (:));
1476 % sldAngErrRel = abs (sldAng / (2 * pi) - 1);
1477 % areaFactUnc = zeros (ay, ax);
1478 % areaFactUnc (2 : ay - 1, 2 : ax - 1) = ... % error estimate based on second-
1479 % ( abs (diff (areaFact (2 : ay - 1, :)', 2)) ) ... % order Taylor expansion
1480 % + abs (diff (areaFact (:, 2 : ax - 1), 2)) ) / 24;
1481 % areaFactUnc ([1 ay], :) = areaFactUnc ([2 ay-1], :); % assume errors at outer edge equal
1482 % areaFactUnc (:, [1 ax]) = areaFactUnc (:, [2 ax-1]); % those of nearest neighbors
1483 intgrnd = areaFact .* gSqr; % to integrate gSqr
1484 % intgrndUnc = zeros (ay, ax); % error estimate for integrand
1485 % intgrndUnc (2 : ay - 1, 2 : ax - 1) = ...
1486 % ( abs (diff (intgrnd (2 : ay - 1, :)', 2)) ) ...
1487 % + abs (diff (intgrnd (:, 2 : ax - 1), 2)) ) / 24;
1488 % intgrndUnc ([1 ay], :) = intgrndUnc ([2 ay-1], :); % assume errors at outer edge equal
1489 % intgrndUnc (:, [1 ax]) = intgrndUnc (:, [2 ax-1]); % those of nearest neighbors
1490 powerVisb = sum (intgrnd (:));
1491 % powerVisbUnc = sum (intgrndUnc (:));
1492 directivityDB = 10 * log10 (4 * pi * gSqrMax / powerVisb);
1493 if beamExist
1494 % sldAngMain = sum (areaFact (beamIdx)); % main beam solid angle
1495 % sldAngMainUnc = sum (areaFactUnc (beamIdx)) + sum (areaFact (beamEdgeIdx)) / 2;
1496 % powerMain = sum (intgrnd (beamIdx)); % power in the main beam
1497 % powerMainUnc = sum (intgrndUnc (beamIdx)) + sum (intgrnd (beamEdgeIdx)) / 2;
1498 % powerSide = sum (intgrnd (sideBool)); % power in the sidelobes
1499 % powerSideUnc = sum (intgrndUnc (:)) - sum (intgrndUnc (beamIdx))...
1500 % + sum (intgrnd (sideEdgeIdx)) / 2;
1501 % sldAngSide = sum (areaFact (sideBool)); % sidelobe equivalent solid angle
1502 % sldAngSideUnc = sum (areaFactUnc (sideBool)) - sum (areaFactUnc (beamIdx)) ...
1503 % + sum (areaFact (sideEdgeIdx)) / 2;
1504 else
1505 % sldAngMain = nan;
1506 % sldAngMainUnc = nan;
1507 % powerMain = nan;
1508 % powerMainUnc = nan;
1509 % powerSide = nan;
1510 % powerSideUnc = nan;
1511 % sldAngSide = nan;
1512 % sldAngSideUnc = nan;
1513 end
1514 % powerMainVisbDB = 10 * log10 (powerMain / powerVisb); % ratio of main beam to visible power
1515 % powerMainVisbUnc = powerMainUnc / powerVisb ...
1516 % + powerMain * powerVisbUnc / powerVisb^2;
1517 % powerVisbSideDB = 10 * log10 (powerVisb / powerSide); % ratio of visible to sidelobe power
1518 % powerVisbSideUnc = powerVisbUnc / powerSide ...
1519 % + powerVisb * powerSideUnc / powerSide^2;
1520 % powerMainSideDB = 10 * log10 (powerMain / powerSide); % ratio of main beam to sidelobe power
1521 % powerMainSideUnc = powerMainUnc / powerSide ...
1522 % + powerMain * powerSideUnc / powerSide^2;
1523 % powerSideAvgDB = 10 * log10 (powerSide / (sldAngSide * gSqrMax)); % average sidelobe power
1524 % powerSideAvgUnc = powerSideUnc / sldAngSide ...
1525 % + powerSide * sldAngSideUnc / sldAngSide^2;
1526 clear intgrnd areaFact areaFactLim tooBig;
1527 clear intgrndUnc areaFactUnc;
1528
1529 % Locate nearest and largest sidelobes
1530 %
1531 % We wish to identify the sidelobe closest in angle to the main beam
1532 % and the sidelobe with the largest peak power. We first find the
1533 % local maxima in the sidelobe region, then for each we determine
1534 % the possible ranges for actual distance from the main beam and
1535 % peak power. (The uncertainties arise from the discrete sampling
1536 % of the array factor.) Using the ranges we select those peaks that
1537 % could possibly be the closest or largest. For each of these
1538 % candidates a more precise location and peak power is computed by
1539 % interpolating over neighboring data. Finally, based on these
1540 % results, the closest and nearest sidelobes are identified.
1541 %
1542 if peakVisb
1543 %
1544 % Find local maxima (sidelobe peaks), using discrete differences

```

```

1545 % to approximate derivatives. The differences are formed from the
1546 % magnitude of the array factor, not the squared magnitude; since
1547 % the behavior should already be parabolic near peaks, squaring
1548 % would produce fourth-order behavior and make second-order
1549 % interpolation less accurate.
1550 %
1551 % Key to the variables below:
1552 % X first differences in x
1553 % Y first differences in y
1554 % XX second differences in x
1555 % YY second differences in y
1556 % X2 first differences in x with double step
1557 % XY cross differences in x and y
1558 % XC nonzero where first difference in x changes sign
1559 % YC nonzero where first difference in y changes sign
1560 %
1561 gMagX = gMag(:, 2:ax) - gMag(:, 1:ax-1);
1562 gMagY = gMag(2:ay, :) - gMag(1:ay-1, :);
1563 gMagXX = [zeros(ay,1) (gMagX(:, 2:ax-1) - gMagX(:, 1:ax-2)) zeros(ay,1)];
1564 gMagYY = [zeros(1,ax); (gMagY(2:ay-1, :) - gMagY(1:ay-2, :))] zeros(1,ax)];
1565 gMagX2 = [zeros(ay,1) (gMag(:, 3:ax) - gMag(:, 1:ax-2))/2 zeros(ay,1)];
1566 gMagXY = [zeros(1,ax); (gMagX2(3:ay, :) - gMagX2(1:ay-2, :))/2; zeros(1,ax)];
1567 gMagXC = [zeros(ay,1) (gMagX(:, 2:ax-1) .* gMagX(:, 1:ax-2) < 0) zeros(ay,1)];
1568 gMagYC = [zeros(1,ax); (gMagY(2:ay-1, :) .* gMagY(1:ay-2, :) < 0); zeros(1,ax)];
1569 slIndx = find ( sideBool ... % identify sidelobe points where
1570 & gMagXC & gMagYC ... % first derivatives change sign,
1571 & (gMagXX < 0) & (gMagYY < 0) ... % second derivatives are negative, and
1572 & (gMagXY.^2 - gMagXX .* gMagYY < 0) ); % discriminant is negative
1573 if isempty (slIndx) % none found?
1574 slIndx = [];
1575 slNrstDist = nan;
1576 slNrstPowrDB = nan;
1577 slNrstVec = nan * ones (1, 3);
1578 slLgstDist = nan;
1579 slLgstPowrDB = nan;
1580 slLgstVec = nan * ones (1, 3);
1581 else % found some peaks
1582 %
1583 % Compute possible ranges of distances and powers; identify
1584 % candidates for closest and largest peaks
1585 %
1586 toward = sign (px - dirCosXmtx (slIndx)) * ay ... % index increment to neighbor
1587 + sign (py - dirCosYmtx (slIndx)); % closer to pointing vector
1588 slCosDistMax = ... % cosine of maximum possible
1589 px * dirCosXmtx (slIndx + toward) ... % angle between pointing
1590 + py * dirCosYmtx (slIndx + toward) ... % vector and each peak;
1591 + pz * dirCosZmtx (slIndx + toward); % dot product
1592 slCosDistMin = ... % likewise for minimum
1593 px * dirCosXmtx (slIndx - toward) ... % possible angle
1594 + py * dirCosYmtx (slIndx - toward) ...
1595 + pz * dirCosZmtx (slIndx - toward);
1596 slNrstBool = (slCosDistMax >= max (slCosDistMin)); % true if peak might be the closest
1597 slPowr = (gMag (slIndx) ... % estimate largest possible
1598 + (-gMagXX (slIndx) ... % interpolated power by adding
1599 + 2 * abs (gMagXY (slIndx)) ... % an error estimate based on the
1600 - gMagYY (slIndx) ) / 8).^2; % differences computed above
1601 slLgstBool = (slPowr >= max (gSqr (slIndx))); % true if peak might be the largest
1602 slCandIndx = slIndx (slNrstBool | slLgstBool); % candidates for closest and largest
1603 numCand = length (slCandIndx); % number of candidates
1604 %
1605 % Interpolate powers and locations for candidates
1606 %
1607 slx = zeros (numCand, 1); % allocate space for x and
1608 sly = zeros (numCand, 1); % y direction cosines
1609 slPowr = zeros (numCand, 1); % and powers
1610 for slPtr = 1 : numCand % loop through candidates
1611 slCol = ceil (slCandIndx (slPtr) / ay); % separate index into column
1612 slRow = slCandIndx (slPtr) - (slCol - 1) * ay; % and row indices
1613 intRad = 1; % interpolation radius
1614 sLOK = 0; % initialize
1615 while ~sLOK & intRad < 3 % no answer yet but too early to bail?
1616 slNbrs = [-intRad : intRad]; % offsets to neighbors
1617 slxFit = dirCosXmtx (slRow + slNbrs, slCol + slNbrs); % x, y, and z coordinates of
1618 slyFit = dirCosYmtx (slRow + slNbrs, slCol + slNbrs); % neighbors (using magnitude,
1619 slzFit = gMag (slRow + slNbrs, slCol + slNbrs); % not power, for z)
1620 slxFit = slxFit (:);
1621 slyFit = slyFit (:);
1622 slzFit = slzFit (:);
1623 slDesMtx = [slxFit.*slxFit/2 slxFit.*slyFit slyFit.*slyFit/2 ... % design matrix
1624 slxFit slyFit ones(size(slxFit))];
1625 [Q, R] = qr (slDesMtx, 0); % now slDesMtx = Q * R; Q' * Q = eye
1626 slPoly = R \ (Q' * slzFit); % solves slDesMtx * slPoly = slzFit
1627 slVec = -[slPoly(1) slPoly(2); slPoly(2) slPoly(3)] ... % find critical point
1628 \ [slPoly(4); slPoly(5)];
1629 sLOK = ... % is interpolated point
1630 (slVec (1) > dirCosX (slCol - intRad)) ... % inside neighborhood?
1631 & (slVec (1) < dirCosX (slCol + intRad)) ... % (pathological cases can
1632 & (slVec (2) > dirCosY (slRow - intRad)) ... % place it outside)
1633 & (slVec (2) < dirCosY (slRow + intRad));
1634 if ~sLOK % outside neighborhood?
1635 intRad = intRad + 1; % yes; cast a wider net
1636 end

```

```

1637         end                                % end interpolation attempts
1638         if sLOK                             % interpolation successful?
1639             slx (slPtr) = slVec (1);         % yes; keep interpolated point
1640             sly (slPtr) = slVec (2);
1641             slPower (slPtr) = ...           % interpolate power
1642             ([slx(slPtr).*slx(slPtr)/2 slx(slPtr).*sly(slPtr) ...
1643             sly(slPtr).*slx(slPtr)/2 slx(slPtr) sly(slPtr) 1] * slPoly).^2;
1644         else                                % interpolation failed
1645             slx (slPtr) = dirCosXmtx (slCandIndx (slPtr)); % use grid location of
1646             sly (slPtr) = dirCosYmtx (slCandIndx (slPtr)); % sampled maximum
1647             slPower (slPtr) = gSqr (slCandIndx (slPtr)); % use sampled power
1648         end
1649     end                                    % end of loop through candidates
1650     %
1651     % Select closest and largest peaks
1652     %
1653     slz = sqrt (1 - slx.^2 - sly.^2);       % z direction cosines
1654     slDist = acos (px * slx + py * sly + pz * slz); % angular distances
1655     [slNrstDist, slNrstIndx] = min (slDist); % smallest distance
1656     slNrstPowerDB = 10 * log10 (slPower (slNrstIndx) / gSqrMax); % and corresponding power
1657     slNrstVec = [slx(slNrstIndx) sly(slNrstIndx) slz(slNrstIndx)]; % keep vector for plotting
1658     [slLgstPowerDB, slLgstIndx] = max (slPower); % largest power
1659     slLgstPowerDB = 10 * log10 (slLgstPowerDB / gSqrMax); % converted to dB
1660     [slLgstDist, slLgstIndx] = min (slDist); % and corresponding distance
1661     slLgstVec = [slx(slLgstIndx) sly(slLgstIndx) slz(slLgstIndx)]; % keep vector
1662     end
1663     else                                    % peak is invisible
1664         slIndx = [];
1665         slNrstDist = nan;
1666         slNrstPowerDB = nan;
1667         slNrstVec = nan * ones (1, 3);
1668         slLgstDist = nan;
1669         slLgstPowerDB = nan;
1670         slLgstVec = nan * ones (1, 3);
1671     end
1672     clear gMagX gMagY gMagXX gMagYY gMagXZ gMagXY gMagXC gMagYC;
1673     clear toward slCosDistMax slCosDistMin;
1674     clear slNrstBool slLgstBool slCandIndx numCand;
1675     clear slx sly slz slPower slPtr slCol slRow intRad sLOK;
1676     clear slNbrs slxFit slyFit slzFit slDesMtx Q R slPoly slVec;
1677     clear slDist slNrstIndx slLgstIndx;
1678     %
1679     % Record characteristics
1680     %
1681     % In order to calculate running means and standard deviations of n
1682     % realizations, we accumulate the mean and variance
1683     %
1684     %      1   n
1685     %      M = - sum x   and
1686     %      n   n m=1   m
1687     %
1688     %      1   n      2
1689     %      V = ---- sum (x - M )
1690     %      n   n - 1 m=1   m   n
1691     %
1692     % using the updating formulas
1693     %
1694     %      x - M
1695     %      n   n-1
1696     %      M = M + ---- and
1697     %      n   n-1   n
1698     %
1699     %      n - 2      1      2
1700     %      V = ---- V + - (x - M ) .
1701     %      n   n - 1 n-1   n   n   n-1
1702     %
1703     % The running mean is simply M(n), and the standard deviation is
1704     % sqrt (V(n)). M is accumulated in the first column of a matrix; V
1705     % in the second. This method is more immune to roundoff error than
1706     % accumulating the sums of values and squares [1].
1707     %
1708     % If the beam is invisibly, the excitations and array factor are
1709     % saved to an automatically-named file.
1710     %
1711     % [1] N. J. Higham, _Accuracy and Stability of Numerical Algorithms_.
1712     % Philadelphia, PA: SIAM, 1996, pp. 12-13.
1713     %
1714     if beamVisib | (numRlz == 1)
1715         if isnan (numAcc (indx))
1716             numAcc (indx) = 1;
1717             pxS (indx, 1) = px;
1718             pxS (indx, 2) = 0;
1719             pyS (indx, 1) = py;
1720             pyS (indx, 2) = 0;
1721             pzS (indx, 1) = pz;
1722             pzS (indx, 2) = 0;
1723             errPointS (indx, 1) = errPoint;
1724             errPointS (indx, 2) = 0;
1725             % errPointUncS (indx, 1) = errPointUnc;
1726             % errPointUncS (indx, 2) = 0;
1727             beamPowerDBS (indx, 1) = beamPowerDB;
1728             beamPowerDBS (indx, 2) = 0;

```



```

1729     beamDepthDBS      (indx, 1) = beamDepthDB;
1730     beamDepthDBS      (indx, 2) = 0;
1731     hpbwMjrS          (indx, 1) = hpbwMjr;
1732     hpbwMjrS          (indx, 2) = 0;
1733     hpbwMnrS          (indx, 1) = hpbwMnr;
1734     hpbwMnrS          (indx, 2) = 0;
1735     rolls             (indx, 1) = roll;
1736     rolls             (indx, 2) = 0;
1737     directivityDBS    (indx, 1) = directivityDB;
1738     directivityDBS    (indx, 2) = 0;
1739     powerMainVisbDBS  (indx, 1) = powerMainVisbDB;
1740     powerMainVisbDBS  (indx, 2) = 0;
1741     powerMainSideDBS  (indx, 1) = powerMainSideDB;
1742     powerMainSideDBS  (indx, 2) = 0;
1743     powerVisbSideDBS  (indx, 1) = powerVisbSideDB;
1744     powerVisbSideDBS  (indx, 2) = 0;
1745     powerSideAvgDBS   (indx, 1) = powerSideAvgDB;
1746     powerSideAvgDBS   (indx, 2) = 0;
1747     slNrstDistS       (indx, 1) = slNrstDist;
1748     slNrstDistS       (indx, 2) = 0;
1749     slNrstPowrDBS     (indx, 1) = slNrstPowrDB;
1750     slNrstPowrDBS     (indx, 2) = 0;
1751     slLgstDistS       (indx, 1) = slLgstDist;
1752     slLgstDistS       (indx, 2) = 0;
1753     slLgstPowrDBS     (indx, 1) = slLgstPowrDB;
1754     slLgstPowrDBS     (indx, 2) = 0;
1755   else
1756     numAcc (indx) = numAcc (indx) + 1;
1757     factV = (numAcc (indx) - 2) / (numAcc (indx) - 1);
1758     dev = px - pxS (indx, 1);
1759     pxS (indx, 2) = pxS (indx, 2) * factV + dev^2 / numAcc (indx);
1760     pxS (indx, 1) = pxS (indx, 1) + dev / numAcc (indx);
1761     dev = py - pyS (indx, 1);
1762     pyS (indx, 2) = pyS (indx, 2) * factV + dev^2 / numAcc (indx);
1763     pyS (indx, 1) = pyS (indx, 1) + dev / numAcc (indx);
1764     dev = pz - pzS (indx, 1);
1765     pzS (indx, 2) = pzS (indx, 2) * factV + dev^2 / numAcc (indx);
1766     pzS (indx, 1) = pzS (indx, 1) + dev / numAcc (indx);
1767     dev = errPoint - errPointS (indx, 1);
1768     errPointS (indx, 2) = errPointS (indx, 2) * factV + dev^2 / numAcc (indx);
1769     errPointS (indx, 1) = errPointS (indx, 1) + dev / numAcc (indx);
1770     % dev = errPointUnc - errPointUncS (indx, 1);
1771     % errPointUncS (indx, 2) = errPointUncS (indx, 2) * factV + dev^2 / numAcc (indx);
1772     % errPointUncS (indx, 1) = errPointUncS (indx, 1) + dev / numAcc (indx);
1773     dev = beamPowerDB - beamPowerDBS (indx, 1);
1774     beamPowerDBS (indx, 2) = beamPowerDBS (indx, 2) * factV + dev^2 / numAcc (indx);
1775     beamPowerDBS (indx, 1) = beamPowerDBS (indx, 1) + dev / numAcc (indx);
1776     dev = beamDepthDB - beamDepthDBS (indx, 1);
1777     beamDepthDBS (indx, 2) = beamDepthDBS (indx, 2) * factV + dev^2 / numAcc (indx);
1778     beamDepthDBS (indx, 1) = beamDepthDBS (indx, 1) + dev / numAcc (indx);
1779     dev = hpbwMjr - hpbwMjrS (indx, 1);
1780     hpbwMjrS (indx, 2) = hpbwMjrS (indx, 2) * factV + dev^2 / numAcc (indx);
1781     hpbwMjrS (indx, 1) = hpbwMjrS (indx, 1) + dev / numAcc (indx);
1782     dev = hpbwMnr - hpbwMnrS (indx, 1);
1783     hpbwMnrS (indx, 2) = hpbwMnrS (indx, 2) * factV + dev^2 / numAcc (indx);
1784     hpbwMnrS (indx, 1) = hpbwMnrS (indx, 1) + dev / numAcc (indx);
1785     dev = roll - rolls (indx, 1);
1786     rolls (indx, 2) = rolls (indx, 2) * factV + dev^2 / numAcc (indx);
1787     rolls (indx, 1) = rolls (indx, 1) + dev / numAcc (indx);
1788     dev = directivityDB - directivityDBS (indx, 1);
1789     directivityDBS (indx, 2) = directivityDBS (indx, 2) * factV + dev^2 / numAcc (indx);
1790     directivityDBS (indx, 1) = directivityDBS (indx, 1) + dev / numAcc (indx);
1791     dev = powerMainVisbDB - powerMainVisbDBS (indx, 1);
1792     powerMainVisbDBS (indx, 2) = powerMainVisbDBS (indx, 2) * factV + dev^2 / numAcc (indx);
1793     powerMainVisbDBS (indx, 1) = powerMainVisbDBS (indx, 1) + dev / numAcc (indx);
1794     dev = powerMainSideDB - powerMainSideDBS (indx, 1);
1795     powerMainSideDBS (indx, 2) = powerMainSideDBS (indx, 2) * factV + dev^2 / numAcc (indx);
1796     powerMainSideDBS (indx, 1) = powerMainSideDBS (indx, 1) + dev / numAcc (indx);
1797     dev = powerVisbSideDB - powerVisbSideDBS (indx, 1);
1798     powerVisbSideDBS (indx, 2) = powerVisbSideDBS (indx, 2) * factV + dev^2 / numAcc (indx);
1799     powerVisbSideDBS (indx, 1) = powerVisbSideDBS (indx, 1) + dev / numAcc (indx);
1800     dev = powerSideAvgDB - powerSideAvgDBS (indx, 1);
1801     powerSideAvgDBS (indx, 2) = powerSideAvgDBS (indx, 2) * factV + dev^2 / numAcc (indx);
1802     powerSideAvgDBS (indx, 1) = powerSideAvgDBS (indx, 1) + dev / numAcc (indx);
1803     dev = slNrstDist - slNrstDistS (indx, 1);
1804     slNrstDistS (indx, 2) = slNrstDistS (indx, 2) * factV + dev^2 / numAcc (indx);
1805     slNrstDistS (indx, 1) = slNrstDistS (indx, 1) + dev / numAcc (indx);
1806     dev = slNrstPowrDB - slNrstPowrDBS (indx, 1);
1807     slNrstPowrDBS (indx, 2) = slNrstPowrDBS (indx, 2) * factV + dev^2 / numAcc (indx);
1808     slNrstPowrDBS (indx, 1) = slNrstPowrDBS (indx, 1) + dev / numAcc (indx);
1809     dev = slLgstDist - slLgstDistS (indx, 1);
1810     slLgstDistS (indx, 2) = slLgstDistS (indx, 2) * factV + dev^2 / numAcc (indx);
1811     slLgstDistS (indx, 1) = slLgstDistS (indx, 1) + dev / numAcc (indx);
1812     dev = slLgstPowrDB - slLgstPowrDBS (indx, 1);
1813     slLgstPowrDBS (indx, 2) = slLgstPowrDBS (indx, 2) * factV + dev^2 / numAcc (indx);
1814     slLgstPowrDBS (indx, 1) = slLgstPowrDBS (indx, 1) + dev / numAcc (indx);
1815   end
1816   else
1817     eval ([ 'save case' sprintf('%0.0f',indx) '-' sprintf('%0.0f',rlzNum) ' exc gSqr' ]);
1818   end
1819   clear factV dev
1820

```

```

1821 % Calculate spherical coordinates of average pointing vector
1822 %
1823 % Let <px>, <py>, and <pz> denote the average direction cosines of
1824 % the pointing vectors, and let vx, vy, and vz denote the
1825 % corresponding variances. We wish to express the direction of the
1826 % average pointing vector [<px> <py> <pz>] in spherical coordinates.
1827 % First, note that the average pointing vector has the norm
1828 %
1829 %      2      2      2
1830 %      p = (<px> + <py> + <pz>) ,
1831 %
1832 % which is less than one if not all realizations are colinear. The
1833 % spherical angles are then given by
1834 %
1835 %      1      2      2 1/2
1836 %      sin pointPolar = - (<px> + <py>) and
1837 %      p
1838 %
1839 %      <py>
1840 %      tan pointAzmth = ---- ,
1841 %      <px>
1842 %
1843 % where we use sin pointPolar instead of the cosine for accuracy
1844 % near boresight.
1845 %
1846 % Also, we wish to estimate the rms angular deviation of a
1847 % realization of the pointing vector from the mean. Adopting an
1848 % unsophisticated method, we add the variances vx and vy to obtain
1849 % an equivalent area in the x-y direction cosine plane, then divide
1850 % the area by cos PointPolar to yield a solid angle on the
1851 % hemisphere. The square root of that area yields the rms angular
1852 % deviation.
1853 %
1854 radSqr = pxS (indx, 1)^2 + pyS (indx, 1)^2;
1855 pointPolar = asin (sqrt (radSqr / (radSqr + pzS (indx, 1)^2)));
1856 pointAzmth = atan2 (pyS (indx, 1), pxS (indx, 1));
1857 if isnan (pointPolar)
1858     pointStdDev = nan;
1859 else
1860     pointStdDev = sqrt ((pxS (indx, 2) + pyS (indx, 2)) / cos (pointPolar));
1861 end
1862 clear radSqr
1863
1864 % Print performance characteristics
1865 %
1866 % Generally, the following statements print the results of the
1867 % analysis followed by the standard deviations of each result in
1868 % curly brackets.
1869 %
1870 if 1 % INPUT 0 to suppress output, 1 to print
1871     fprintf (1, '\nMeans and [std devs] for %0.0f of %0.0f realizations\n', rlzNum, numRlz);
1872     fprintf (1, 'beam direction : (%0.3f, %0.3f) deg, std dev %0.3f deg\n', ...
1873         pointPolar / rpd, (pointAzmth + azmthOffst) / rpd, pointStdDev / rpd);
1874     fprintf (1, 'pointing error : %8.4f [%0.4f] deg\n', ...
1875         errPointS (indx, 1) / rpd, sqrt (errPointS (indx, 2)) / rpd);
1876 % fprintf (1, 'pntng error unc: %8.4f [%0.4f] deg (2 sigma)\n', ...
1877 %     2 * errPointUncS (indx, 1) / rpd, 2 * sqrt (errPointUncS (indx, 2)) / rpd);
1878     fprintf (1, 'peak power dens: %7.3f [%0.3f] dB\n', ...
1879         beamPowerDBS (indx, 1), sqrt (beamPowerDBS (indx, 2)));
1880     fprintf (1, 'beam depth : %6.2f [%0.2f] dB re peak\n', ...
1881         beamDepthDBS (indx, 1), sqrt (beamDepthDBS (indx, 2)));
1882     fprintf (1, 'beam width : (%6.3f [%0.3f], %0.3f [%0.3f]) deg\n', ...
1883         hpbwMjrS (indx, 1) / rpd, sqrt (hpbwMjrS (indx, 2)) / rpd, ...
1884         hpbwMnrS (indx, 1) / rpd, sqrt (hpbwMnrS (indx, 2)) / rpd);
1885     fprintf (1, 'beam roll : %6.2f [%0.2f] deg\n', ...
1886         (rollS (indx, 1) + azmthOffst) / rpd, sqrt (rollS (indx, 2)) / rpd);
1887     fprintf (1, 'directivity : %7.3f [%0.3f] dB\n', ...
1888         directivityDBS (indx, 1), sqrt (directivityDBS (indx, 2)));
1889     fprintf (1, 'power ratio m/v: %7.3f [%0.3f] dB\n', ...
1890         powerMainVisbDBS (indx, 1), sqrt (powerMainVisbDBS (indx, 2)));
1891     fprintf (1, 'power ratio m/s: %7.3f [%0.3f] dB\n', ...
1892         powerMainSideDBS (indx, 1), sqrt (powerMainSideDBS (indx, 2)));
1893     fprintf (1, 'power ratio v/s: %7.3f [%0.3f] dB\n', ...
1894         powerVisbSideDBS (indx, 1), sqrt (powerVisbSideDBS (indx, 2)));
1895     fprintf (1, 'avg sidelobe : %6.2f [%0.2f] dB re peak\n', ...
1896         powerSideAvgDBS (indx, 1), sqrt (powerSideAvgDBS (indx, 2)));
1897     fprintf (1, 'nrst sidelobe : %6.2f [%0.2f] dB re peak, %0.2f [%0.2f] deg off beam\n', ...
1898         slNrstPowrDBS (indx, 1), sqrt (slNrstPowrDBS (indx, 2)), ...
1899         slNrstDistS (indx, 1) / rpd, sqrt (slNrstDistS (indx, 2)) / rpd);
1900     fprintf (1, 'lgst sidelobe : %6.2f [%0.2f] dB re peak, %0.2f [%0.2f] deg off beam\n', ...
1901         slLgstPowrDBS (indx, 1), sqrt (slLgstPowrDBS (indx, 2)), ...
1902         slLgstDistS (indx, 1) / rpd, sqrt (slLgstDistS (indx, 2)) / rpd);
1903 end
1904
1905 end % loop over realizations
1906
1907 % Plot performance characteristics as function of independent variable
1908 % (summary plot).
1909 %
1910 % If more than one realization has been accumulated for any value of
1911 % the independent variable, the mean is plotted with uncertainty bars.
1912 % The extension of the uncertainty bar above the mean equals one

```

```

1913 % standard deviation, and likewise below the mean. Otherwise, only
1914 % the values for the one realization are plotted.
1915 %
1916 % Plots that show more than one measure distinguish them by color or
1917 % line style and may use both a left and right axis. The color or
1918 % style and axis for each measure is given in codes in parentheses in
1919 % the title of the plot. The first code abbreviates the color or line
1920 % style:
1921 %
1922 %   R red      - solid
1923 %   G green    -- dashed
1924 %   B blue     : dotted
1925 %   C cyan
1926 %   M magenta
1927 %   Y yellow
1928 %   K black
1929 %   W white
1930 %
1931 % and the second letter indicates the axis, L for left and R for
1932 % right.
1933 %
1934 if indVarLen > 1
1935     figure (figSum);
1936     clf;
1937     axesSum = zeros (12, 1); % space for axes handles
1938     %
1939     % Axes 1: pointing error
1940     %
1941     subplot (4, 2, 1);
1942     axesSum (1) = gca;
1943     if any (numAcc > 1)
1944         hline = errorbar (indVar, errPoints (:, 1) / rpd, sqrt (errPoints (:, 2)) / rpd);
1945         set (hline, discrim, discrimValue {1}); % possibly override errorbar's default solid line style
1946         set (hline (1), 'linestyle', '-'); % but leave the error bars themselves solid
1947     else
1948         plot (indVar, errPoints (:, 1) / rpd);
1949     end
1950     ylabel ('(deg)');
1951     title ('pointing error');
1952     %
1953     % Axes 2 and 3: beam power and directivity
1954     %
1955     subplot (4, 2, 2);
1956     axesSum (2) = gca;
1957     if any (numAcc > 1)
1958         hline = errorbar (indVar, beamPowerDBS (:, 1), sqrt (beamPowerDBS (:, 2)));
1959         set (hline, discrim, discrimValue {1});
1960         set (hline (1), 'linestyle', '-');
1961     else
1962         plot (indVar, beamPowerDBS (:, 1));
1963     end
1964     ylabel ('(dB re coherent)');
1965     title (strcat ('peak power dens (', discrimName {1}, ...
1966                   ' L), directivity (', discrimName {2}, ' R)'));
1967     axesSum (3) = axes ('position', get (gca, 'position'));
1968     if any (numAcc > 1)
1969         hline = errorbar (indVar, directivityDBS (:, 1), sqrt (directivityDBS (:, 2)));
1970         set (hline, discrim, discrimValue {2});
1971         set (hline (1), 'linestyle', '-');
1972     else
1973         plot (indVar, directivityDBS (:, 1), discrim, discrimValue {2});
1974     end
1975     set (gca, 'yAxisLocation', 'right', 'color', 'none');
1976     %
1977     % Axes 4 and 5: beam widths
1978     %
1979     subplot (4, 2, 3);
1980     axesSum (4) = gca;
1981     if any (numAcc > 1)
1982         hline = errorbar (indVar, hpbwMjrS (:, 1) / rpd, sqrt (hpbwMjrS (:, 2)) / rpd);
1983         set (hline, discrim, discrimValue {1});
1984         set (hline (1), 'linestyle', '-');
1985     else
1986         plot (indVar, hpbwMjrS (:, 1) / rpd);
1987     end
1988     ylabel ('(deg)');
1989     title (strcat ('hpbw major (', discrimName {1}, ...
1990                   ' L) & minor (', discrimName {2}, ' R)'));
1991     axesSum (5) = axes ('position', get (gca, 'position'));
1992     if any (numAcc > 1)
1993         hline = errorbar (indVar, hpbwMnrS (:, 1) / rpd, sqrt (hpbwMnrS (:, 2)) / rpd);
1994         set (hline, discrim, discrimValue {2});
1995         set (hline (1), 'linestyle', '-');
1996     else
1997         plot (indVar, hpbwMnrS (:, 1) / rpd, discrim, discrimValue {2});
1998     end
1999     set (gca, 'yAxisLocation', 'right', 'color', 'none');
2000     yLimL = get (axesSum (4), 'ylim');
2001     yLimR = get (axesSum (5), 'ylim');
2002     if yLimL (1) < yLimR (2)
2003         set (axesSum (4), 'xlimmode', 'manual', 'ylim', [yLimR (1) yLimL (2)]);
2004         set (axesSum (5), 'xlimmode', 'manual', 'ylim', [yLimR (1) yLimL (2)]);

```

```

2005     % Setting xlimmode to manual prevents rescaling of the x axis when
2006     % the y axis is changed.
2007 end
2008 %
2009 % Axes 6: beam roll
2010 %
2011 subplot (4, 2, 4);
2012 axesSum (6) = gca;
2013 if any (numAcc > 1)
2014     hline = errorbar (indVar, rollS (:, 1) / rpd, sqrt (rollS (:, 2)) / rpd);
2015     set (hline, discrim, discrimValue {1});
2016     set (hline (1), 'linestyle', '-');
2017 else
2018     plot (indVar, rollS (:, 1) / rpd);
2019 end
2020 ylabel ('(deg)');
2021 title ('beam roll');
2022 %
2023 % Axes 7: beam depth
2024 %
2025 subplot (4, 2, 5);
2026 axesSum (7) = gca;
2027 if any (numAcc > 1)
2028     hline = errorbar (indVar, beamDepthDBS (:, 1), sqrt (beamDepthDBS (:, 2)));
2029     set (hline, discrim, discrimValue {1});
2030     set (hline (1), 'linestyle', '-');
2031 else
2032     plot (indVar, beamDepthDBS (:, 1));
2033 end
2034 ylabel ('(dB re peak)');
2035 title ('beam depth');
2036 %
2037 % Axes 8 and 9: power ratios
2038 %
2039 subplot (4, 2, 6);
2040 axesSum (8) = gca;
2041 if any (numAcc > 1)
2042     hline = errorbar (indVar, powerMainVisbDBS (:, 1), sqrt (powerMainVisbDBS (:, 2)));
2043     set (hline, discrim, discrimValue {1});
2044     set (hline (1), 'linestyle', '-');
2045 else
2046     plot (indVar, powerMainVisbDBS (:, 1));
2047 end
2048 ylabel ('(dB)');
2049 title (strcat ('Power m/v (' , discrimValue {1}, ...
2050               ' L), m/s (' , discrimValue {2}, ...
2051               ' R), v/s (' , discrimValue {3}, ' R)'));
2052 axesSum (9) = axes ('position', get (gca, 'position'));
2053 if any (numAcc > 1)
2054     hline = errorbar (indVar, powerMainSideDBS (:, 1), ...
2055                     sqrt (powerMainSideDBS (:, 2)));
2056     set (hline, discrim, discrimValue {2});
2057     set (hline (1), 'linestyle', '-');
2058     set (gca, 'nextplot', 'add');
2059     hline = errorbar (indVar, powerVisbSideDBS (:, 1), ...
2060                     sqrt (powerVisbSideDBS (:, 2)));
2061     set (hline, discrim, discrimValue {3});
2062     set (hline (1), 'linestyle', '-');
2063     set (gca, 'nextplot', 'replace');
2064 else
2065     plot (indVar, powerMainSideDBS (:, 1), discrim, discrimValue {2});
2066     set (gca, 'nextplot', 'add');
2067     plot (indVar, powerVisbSideDBS (:, 1), discrim, discrimValue {3});
2068     set (gca, 'nextplot', 'replace');
2069 end
2070 set (gca, 'yAxisLocation', 'right', 'color', 'none');
2071 %
2072 % Axes 10 and 11: sidelobe powers
2073 %
2074 subplot (4, 2, 7);
2075 axesSum (10) = gca;
2076 if any (numAcc > 1)
2077     hline = errorbar (indVar, slLgstPowrDBS (:, 1), sqrt (slLgstPowrDBS (:, 2)));
2078     set (hline, discrim, discrimValue {1});
2079     set (hline (1), 'linestyle', '-');
2080     set (gca, 'nextplot', 'add');
2081     hline = errorbar (indVar, slNrstPowrDBS (:, 1), sqrt (slNrstPowrDBS (:, 2)));
2082     set (hline, discrim, discrimValue {2});
2083     set (hline (1), 'linestyle', '-');
2084     set (gca, 'nextplot', 'replace');
2085 else
2086     plot (indVar * ones (1, 2), ...
2087         [slLgstPowrDBS (:, 1) slNrstPowrDBS (:, 1)]);
2088 end
2089 ylabel ('(dB re peak)');
2090 title (strcat ('sidelobe power: lgst (' , discrimValue {1}, ...
2091               ' L), nrst (' , discrimValue {2}, ...
2092               ' L), avg (' , discrimValue {3}, ' R)'));
2093 axesSum (11) = axes ('position', get (gca, 'position'));
2094 if any (numAcc > 1)
2095     hline = errorbar (indVar, powerSideAvgDBS (:, 1), sqrt (powerSideAvgDBS (:, 2)));
2096     set (hline, discrim, discrimValue {3});

```

```

2097     set (hline (1), 'linestyle', '-');
2098 else
2099     plot (indVar, powerSideAvgDBS (:, 1), discrim, discrimValue {3});
2100 end
2101 set (gca, 'yAxisLocation', 'right', 'color', 'none');
2102 %
2103 % Axes 12: sidelobe distances
2104 %
2105 subplot (4, 2, 8);
2106 axesSum (12) = gca;
2107 if any (numAcc > 1)
2108     hline = errorbar (indVar, slLgstDistS (:, 1) / rpd, sqrt (slLgstDistS (:, 2)) / rpd);
2109     set (hline, discrim, discrimValue {1});
2110     set (hline (1), 'linestyle', '-');
2111     set (gca, 'nextplot', 'add');
2112     hline = errorbar (indVar, slNrstDistS (:, 1) / rpd, sqrt (slNrstDistS (:, 2)) / rpd);
2113     set (hline, discrim, discrimValue {2});
2114     set (hline (1), 'linestyle', '-');
2115     set (gca, 'nextplot', 'replace');
2116 else
2117     plot (indVar * ones (1, 2), ...
2118         [slLgstDistS(:,1) slNrstDistS(:,1)] / rpd);
2119 end
2120 ylabel ('(deg)');
2121 title (strcat ('sidelobe distance: lgst (' , discrimValue {1}, ...
2122             ', nrst (' , discrimValue {2}, ')'));
2123 %
2124 % Touch up
2125 %
2126 set (findobj (gcf, 'type', 'axes'), 'xlim', ... % make x-axis limits uniform
2127     [min(indVar) max(indVar)] ...
2128     + 0.1 * (max (indVar) - min (indVar)) * [-1 1]);
2129 axesSumTitle = axes ('position', [0 0 1 1], ... % create invisible axes
2130     'color', 'none', 'visible', 'off', ... % for titling
2131     'defaultFontSize', 10, ...
2132     'defaultTextHorizontalAlignment', 'center');
2133 text (0.5, 0.05, indVarName, ... % display name of independent
2134     'horizontalAlignment', 'center'); % variable
2135 end
2136 clear hline
2137 %
2138 % Plot last realization
2139 %
2140 % Three projections of the hemisphere are available: Lambert,
2141 % stereographic, and orthographic.
2142 %
2143 % Lambert projection:
2144 %
2145 % The Lambert projection preserves the relative areas of portions of
2146 % the hemisphere. That is, the ratio of areas of two regions on the
2147 % projection is the same as on the hemisphere. The azimuth coordinate
2148 % of a point in the projection is the same as its azimuth coordinate
2149 % on the hemisphere, while its radius  $r$  from the center of the
2150 % projection is related to the polar angle. This relationship may be
2151 % derived by setting the spherical surface area  $\sin$  polar  $d(\text{polar})$ 
2152 %  $d(\text{azmth})$  equal to a constant times the planar surface area  $r$   $dr$ 
2153 %  $d(\text{azmth})$  and integrating. The radius is then given by
2154 %
2155 % 
$$r = 2 \int_0^{\text{polar}} \sin \theta d\theta$$

2156 %
2157 %
2158 % For computer graphics the Cartesian coordinates are more convenient;
2159 % they are
2160 %
2161 %  $u = r \cos \text{azmth} = R \text{ cx}$ 
2162 %
2163 %  $v = r \sin \text{azmth} = R \text{ cy}$ 
2164 %
2165 % where
2166 %
2167 % 
$$R = 2 \int_0^{\text{polar}} \sec^2 \theta d\theta = (1 + \text{cz})$$

2168 %
2169 %
2170 % For points outside visible space (that is, for  $\text{cx}^2 + \text{cy}^2 > 1$ ),  $\text{cz}$ 
2171 % is zero so that  $R = 1$  and no transformation is applied.
2172 %
2173 % Stereographic projection:
2174 %
2175 % The stereographic projection preserves angles on the hemisphere. To
2176 % derive the governing relationship for the projection, use the same
2177 % azimuthal angle for the projection as for the hemisphere, and let
2178 % the radius be a function of the polar angle:  $r = f(\text{polar})$ . Equate
2179 % the aspect ratios of orthogonal derivatives, as
2180 %
2181 % 
$$\frac{d(\text{polar})}{\sin \text{polar} d(\text{azmth})} = \frac{dr}{r d(\text{azmth})}$$

2182 %
2183 %
2184 %
2185 %
2186 %

```

```

2187 % f'(polar) d(polar)
2188 % = -----
2189 % f (polar) d(azmth)
2190 %
2191 % (where f' is the first derivative), rearrange, and integrate to
2192 % obtain
2193 %
2194 % polar 1 - cos polar
2195 % f (polar) = tan ----- = ----- ,
2196 % 2 sin polar
2197 %
2198 % up to an arbitrary multiplicative constant. The projected Cartesian
2199 % coordinates of a point (cx, cy, cz) on the sphere are
2200 %
2201 % u = r cos azmth = R cx
2202 %
2203 % v = r sin azmth = R cy
2204 %
2205 % where
2206 %
2207 % f (polar) 1 1
2208 % R = ----- = ----- = ----- .
2209 % sin polar 1 + cos polar 1 + cz
2210 %
2211 % For points outside visible space (that is, for cx^2 + cy^2 > 1), cz
2212 % is zero so that R = 1 and no transformation is applied.
2213 %
2214 % The center of projection is opposite boresight (cx = cy = 0, cz =
2215 % -1), and with the above choice of multiplicative constant, the plane
2216 % of projection is the cz = 0 plane.
2217 %
2218 % Orthographic projection:
2219 %
2220 % The orthographic projection gives a 3D view of the hemisphere.
2221 %
2222 if 1 % INPUT 1 to plot, 0 to skip
2223 proj = 1; % INPUT 1 for 2D equal-area Lambert
2224 % 2 for 2D stereographic
2225 % 3 for orthographic (3D hemisphere)
2226 coordSys = 1; % INPUT 1 for grid of spherical coordinates
2227 % 2 for grid of traditional coordinates
2228 faceColor = 'flat'; % INPUT 'flat' or 'interp' shading
2229 pointZoom = 0; % INPUT magnification factor or 0 for centered full view
2230 % The "show" inputs below are coded only for 2D views.
2231 showBeamRegion = 0; % INPUT 1 to show main beam region
2232 showWidthRegion = 0; % region above width contour
2233 showWidthContAct = 0; % actual width contour
2234 showWidthContFit = 0; % fitted width contour (ellipse)
2235 showPointGrid = 0; % main beam peak on sampled grid
2236 showPoint = 1; % interpolated main beam peak (pointing vector)
2237 showPointUnc = 0; % axes of uncertainty ellipse of pointing vector
2238 showSidelobeGrid = 0; % sidelobe peaks on sampled grid
2239 showSidelobeNrst = 1; % nearest sidelobe
2240 showSidelobeLgst = 1; % largest sidelobe
2241 %
2242 % Prepare for plotting
2243 %
2244 if strcmp (faceColor, 'interp')
2245 dirCosXmtxSurf = dirCosXmtx; % use true grid
2246 dirCosYmtxSurf = dirCosYmtx;
2247 dirCosZmtxSurf = dirCosZmtx;
2248 visBoolSurf = visBool ;
2249 elseif strcmp (faceColor, 'flat')
2250 dirCosXmtxSurf = ones (ay, 1) * dirCosShiftX; % use shifted grid to center
2251 dirCosYmtxSurf = dirCosShiftY * ones (1, ax); % patches on data points
2252 radSqr = dirCosXmtxSurf.^2 + dirCosYmtxSurf.^2;
2253 visBoolSurf = (radSqr < 1);
2254 dirCosZmtxSurf = zeros (ay, ax);
2255 dirCosZmtxSurf (visBoolSurf) = sqrt (1 - radSqr (visBoolSurf));
2256 clear radSqr;
2257 else
2258 error ('Illegal value of faceColor.');
```

```

2279     gPlot = zeros (ay, ax);
2280     clim = [-50 0]; % INPUT dB range
2281     gPlot (gOKIndx) = max (clim (1), 10 * log10 (gSqr (gOKIndx)));
2282     gPlot (gZeroIndx) = clim (1) * ones (size (gZeroIndx)); % condition log of 0
2283 else
2284     % Linear plot
2285     gPlot = gSqr;
2286     clim = [0 1];
2287 end
2288 if invertBkgd % set appropriate value for invisible points
2289     gPlot (gBlkIndx) = clim (2) * ones (size (gBlkIndx));
2290 else
2291     gPlot (gBlkIndx) = clim (1) * ones (size (gBlkIndx));
2292 end
2293 clear visBoolSurf gBlkIndx gZeroIndx gOKIndx;
2294 figure (figPat);
2295 fore = get (figPat, 'defaultLineColor'); % expect black or white
2296 if invertBkgd % choose fore- and background colors compatible with color map
2297     fore = 1 - fore; % swap
2298 end
2299 back = 1 - fore;
2300 switch coordSys
2301     case 1
2302         grid1Polar = (0 : 10 : 90) * rpd; % lines of constant polar angle
2303         grid1Azmth = (0 : 5 : 360) * rpd - azmthOffst;
2304         grid2Polar = (0 : 5 : 90) * rpd; % lines of constant azimuth
2305         grid2Azmth = (0 : 30 : 360) * rpd - azmthOffst;
2306         [grid1Polar, grid1Azmth] = meshgrid (grid1Polar, grid1Azmth);
2307         [grid2Azmth, grid2Polar] = meshgrid (grid2Azmth, grid2Polar);
2308     case 2
2309         grid1Az = (-90 : 10 : 90) * rpd; % lines of constant azimuth
2310         grid1El = (-90 : 5 : 90) * rpd;
2311         grid2Az = (-90 : 10 : 90) * rpd; % lines of constant elevation
2312         grid2El = (-90 : 10 : 90) * rpd;
2313         [grid1Az, grid1El] = meshgrid (grid1Az, grid1El);
2314         [grid2El, grid2Az] = meshgrid (grid2El, grid2Az);
2315         grid1Polar = acos (cos (grid1El) .* cos (grid1Az));
2316         grid1Azmth = atan2 (tan (grid1El), -sin (grid1Az)) - azmthOffst;
2317         grid2Polar = acos (cos (grid2El) .* cos (grid2Az));
2318         grid2Azmth = atan2 (tan (grid2El), -sin (grid2Az)) - azmthOffst;
2319     otherwise
2320         error ('Invalid value of coordSys.');
```

```

2321 end
2322 %
2323 % Plot array factor
2324 %
2325 if proj == 1
2326     %
2327     % Lambert projection
2328     %
2329     radFactSurf = 1 ./ sqrt (1 + dirCosZMtxSurf); % radius factor for surface plot
2330     hSurf = surf (radFactSurf .* dirCosXMTxSurf, ...
2331         radFactSurf .* dirCosYMTxSurf, gPlot);
2332     grid1RadFact = sqrt (2) * sin (grid1Polar / 2);
2333     line (grid1RadFact .* cos (grid1Azmth), ...
2334         grid1RadFact .* sin (grid1Azmth), ...
2335         clim (2) * ones (size (grid1RadFact)), 'color', fore);
2336     grid2RadFact = sqrt (2) * sin (grid2Polar / 2);
2337     line (grid2RadFact .* cos (grid2Azmth), ...
2338         grid2RadFact .* sin (grid2Azmth), ...
2339         clim (2) * ones (size (grid2RadFact)), 'color', fore);
2340     set (gca, 'drawmode', 'fast'); % no hidden objects to worry about
2341     xylim = [-1 1];
2342     zlim = clim;
2343     viewAz = 0; % Matlab azimuth and
2344     viewEl = 90 * rpd; % elevation (but in radians)
2345 elseif proj == 2
2346     %
2347     % Stereographic projection
2348     %
2349     radFactSurf = 1 ./ (1 + dirCosZMtxSurf); % radius factor for surface plot
2350     hSurf = surf (radFactSurf .* dirCosXMTxSurf, ...
2351         radFactSurf .* dirCosYMTxSurf, gPlot);
2352     grid1RadFact = tan (grid1Polar / 2);
2353     line (grid1RadFact .* cos (grid1Azmth), ...
2354         grid1RadFact .* sin (grid1Azmth), ...
2355         clim (2) * ones (size (grid1RadFact)), 'color', fore);
2356     grid2RadFact = tan (grid2Polar / 2);
2357     line (grid2RadFact .* cos (grid2Azmth), ...
2358         grid2RadFact .* sin (grid2Azmth), ...
2359         clim (2) * ones (size (grid2RadFact)), 'color', fore);
2360     set (gca, 'drawmode', 'fast'); % no hidden objects to worry about
2361     xylim = [-1 1];
2362     zlim = clim;
2363     viewAz = 0; % Matlab azimuth and
2364     viewEl = 90 * rpd; % elevation (but in radians)
2365 elseif proj == 3
2366     %
2367     % Orthographic projection (3D hemisphere)
2368     %
2369     float = 1.02; % radius of annotations relative to unit hemisphere
2370     hSurf = surf (dirCosXMTxSurf, dirCosYMTxSurf, dirCosZMtxSurf, gPlot);

```

```

2371     grid1RadFact = sin (grid1Polar);
2372     line (grid1RadFact .* cos (grid1Azmth) * float, ...
2373           grid1RadFact .* sin (grid1Azmth) * float, ...
2374           cos (grid1Polar) * float, 'color', fore);
2375     grid2RadFact = sin (grid2Polar);
2376     line (grid2RadFact .* cos (grid2Azmth) * float, ...
2377           grid2RadFact .* sin (grid2Azmth) * float, ...
2378           cos (grid2Polar) * float, 'color', fore);
2379     set (gca, 'drawmode', 'normal'); % remove hidden objects
2380     xylim = [-1 1] * float;
2381     zlim = [-1 1] * float;
2382     switch 1 % INPUT 1 to look down main beam; 2, down boresight; 3, custom
2383     case 1
2384         % Look down main beam
2385         viewAz = pi/2 + steerAzmth + azmthOffst; % Matlab azimuth and
2386         viewEl = pi/2 - steerPolar; % elevation (but in radians)
2387     case 2
2388         % Look down boresight
2389         viewAz = 0; % Matlab azimuth and
2390         viewEl = 90 * rpd; % elevation (but in radians)
2391         set (gca, 'drawmode', 'fast'); % no hidden surfaces
2392     otherwise
2393         % Look somewhere
2394         viewAz = 60 * rpd; % INPUT custom view azimuth
2395         viewEl = 30 * rpd; % and elevation (Matlab coordinates)
2396     end
2397     end % plotting
2398     %
2399     % Annotate plot (2D only)
2400     %
2401     if (proj == 1) | (proj == 2)
2402         switch proj % set appropriate radius factor
2403         case 1
2404             radFact = 1 ./ sqrt (1 + dirCosZMtx);
2405         case 2
2406             radFact = 1 ./ (1 + dirCosZMtx);
2407         end
2408         if showBeamRegion & beamExist
2409             line (radFact (beamIndx) .* dirCosXMtx (beamIndx), ...
2410                   radFact (beamIndx) .* dirCosYmtx (beamIndx), ...
2411                   clim (2) * ones (size (beamIndx)), ...
2412                   'linestyle', 'none', 'marker', '+', 'color', fore);
2413         end
2414         if showWidthRegion & capClosed
2415             line (radFact (capIndx) .* dirCosXMtx (capIndx), ...
2416                   radFact (capIndx) .* dirCosYmtx (capIndx), ...
2417                   clim (2) * ones (size (capIndx)), ...
2418                   'linestyle', 'none', 'marker', 'x', 'color', fore);
2419         end
2420         if showWidthContAct & capClosed
2421             switch proj
2422             case 1
2423                 radFactCapAct = 1 ./ sqrt (1 + capContZ);
2424             case 2
2425                 radFactCapAct = 1 ./ (1 + capContZ);
2426             end
2427             line (radFactCapAct .* capContX, radFactCapAct .* capContY, ...
2428                   clim (2) * ones (size (capContX)), 'linestyle', ':', 'color', back);
2429             clear radFactCapAct
2430         end
2431         if showWidthContFit & capClosed
2432             switch proj
2433             case 1
2434                 radFactCapFit = 1 ./ sqrt (1 + cFitZ);
2435             case 2
2436                 radFactCapFit = 1 ./ (1 + cFitZ);
2437             end
2438             line (radFactCapFit .* cFitX, radFactCapFit .* cFitY, ...
2439                   clim (2) * ones (size (cFitX)), 'linestyle', '-', 'color', back);
2440             clear radFactCapFit
2441         end
2442         if showPointGrid
2443             line (radFact (gSqrMaxRow, gSqrMaxCol) .* dirCosXMtx (gSqrMaxRow, gSqrMaxCol), ...
2444                   radFact (gSqrMaxRow, gSqrMaxCol) .* dirCosYmtx (gSqrMaxRow, gSqrMaxCol), ...
2445                   clim (2), 'linestyle', 'none', 'marker', '*', 'color', back);
2446         end
2447         if showPointUnc
2448             switch proj
2449             case 1
2450                 pointRadFact = 1 / sqrt (1 + pz);
2451                 Jacob = [1+pz+px^2/pz px*py/pz % Jacobian of
2452                         py*px/pz 1+pz+py^2/pz] / (2*(1+pz)^(3/2)); % projection
2453             case 2
2454                 pointRadFact = 1 / (1 + pz);
2455                 Jacob = [1+pz+px^2/pz px*py/pz % Jacobian of
2456                         py*px/pz 1+pz+py^2/pz] / (1+pz)^2; % projection
2457             end
2458             pVarProj = Jacob * pVar * Jacob'; % covariance matrix in this projection
2459             [pEigVec, pEigVal] ... % diagonalize: pVar
2460             = eig (pVarProj); % = pEigVec * pEigVal * pEigVec'
2461             pPrAx = 2 * pEigVec ... % scale principal axes (columns of
2462                   * sqrt (pEigVal); % pEigVec) to 2 standard deviations

```



```

2463     line (pointRadFact * px + [-1 1]' * pPrAx (1, :), ...
2464           pointRadFact * py + [-1 1]' * pPrAx (2, :), ...
2465           clim (2) * [1 1], ...
2466           'linestyle', '-', 'color', back);
2467     clear pointRadFact Jacob pVarProj pEigVec pEigVal pPrAx
2468   elseif showPoint
2469     switch proj
2470     case 1
2471       pointRadFact = 1 / sqrt (1 + pz);
2472     case 2
2473       pointRadFact = 1 / (1 + pz);
2474     end
2475     line (pointRadFact * px, pointRadFact * py, clim (2), ...
2476           'linestyle', 'none', 'marker', '.', 'color', back)
2477     clear pointRadFact
2478   end
2479   if showSidelobeGrid
2480     line (radFact (slIndx) .* dirCosXmtx (slIndx), ...
2481           radFact (slIndx) .* dirCosYmtx (slIndx), ...
2482           clim (2) * ones (size (slIndx)), ...
2483           'linestyle', 'none', 'marker', 's', 'color', back);
2484   end
2485   if showSidelobeNrst
2486     switch proj
2487     case 1
2488       radFactSlNrst = 1 / sqrt (1 + slNrstVec (3));
2489     case 2
2490       radFactSlNrst = 1 / (1 + slNrstVec (3));
2491     end
2492     line (radFactSlNrst .* slNrstVec (1), ...
2493           radFactSlNrst .* slNrstVec (2), ...
2494           clim (2), 'linestyle', 'none', 'marker', '+', 'color', back);
2495     clear radFactSlNrst
2496   end
2497   if showSidelobeLgst
2498     switch proj
2499     case 1
2500       radFactSlLgst = 1 / sqrt (1 + slLgstVec (3));
2501     case 2
2502       radFactSlLgst = 1 / (1 + slLgstVec (3));
2503     end
2504     line (radFactSlLgst .* slLgstVec (1), ...
2505           radFactSlLgst .* slLgstVec (2), ...
2506           clim (2), 'linestyle', 'none', 'marker', 'x', 'color', back);
2507     clear radFactSlLgst
2508   end
2509   end % annotations
2510   %
2511   % Arrange graphics properties
2512   %
2513   axesPat = gca;
2514   rotate (get (axesPat, 'children'), ... % rotate plotted objects to
2515           [0 0 1], azmthOffset / rpd); % compensate for azmthOffset
2516   set (hSurf, 'edgecolor', 'none');
2517   set (hSurf, 'facecolor', faceColor);
2518   colormap (cmap);
2519   set (axesPat, 'clim', clim);
2520   if cbarVert % position the colorbar
2521     axesCbar = colorbar ('vert');
2522     set (axesCbar, ...
2523           'units', 'normalized', ...
2524           'position', [(1+0.2*cbarSize)/(1+cbarSize) 0.05 0.4*cbarSize/(1+cbarSize) 0.9]);
2525     set (axesPat, ...
2526           'units', 'normalized', ...
2527           'position', [0 0 1/(1+cbarSize) 1]);
2528   else
2529     axesCbar = colorbar ('horiz');
2530     set (axesCbar, ...
2531           'units', 'normalized', ...
2532           'position', [0.05 0.3*cbarSize/(1+cbarSize) 0.9 0.5*cbarSize/(1+cbarSize)]);
2533     set (axesPat, ...
2534           'units', 'normalized', ...
2535           'position', [0 cbarSize/(1+cbarSize) 1 1/(1+cbarSize)]);
2536   end
2537   set (figPat, 'children', ... % put color bar in front of pattern but let
2538         [axesCbar axesPat]); % axesPat remain the current axis
2539   set (axesPat, ...
2540         'xlim', ylim, ...
2541         'ylim', ylim, ...
2542         'zlim', zlim, ...
2543         'dataAspectRatio', diff ({xlim' ylim' zlim'}), ...
2544         'visible', 'off', ...
2545         'view', [viewAz/rpd viewEl/rpd]);
2546   if proj == 3
2547     cameraDist = norm ( ... % distance from camera
2548                       get (axesPat, 'cameraPosition') ... % to the surface
2549                       - get (axesPat, 'cameraTarget'), 2);
2550     set (axesPat, 'cameraViewAngle', ... % set view angle to
2551           2 * atan (float * diff (zlim) ... % exactly span the
2552                     / (cameraDist * diff (ylim))) / rpd); % unit sphere
2553   end
2554   if (pointZoom ~= 0) & peakVisb

```

```

2555     pxRot = cos (azmthOffst) * px - sin (azmthOffst) * py; % compensate for
2556     pyRot = sin (azmthOffst) * px + cos (azmthOffst) * py; % azmthOffst
2557     if proj == 1
2558         pointRadFact = 1 / sqrt (1 + pz);
2559         set (axesPat, 'xlim', pointRadFact * pxRot + [-1 1] / pointZoom, ...
2560             'ylim', pointRadFact * pyRot + [-1 1] / pointZoom);
2561     elseif proj == 2
2562         pointRadFact = 1 / (1 + pz);
2563         set (axesPat, 'xlim', pointRadFact * pxRot + [-1 1] / pointZoom, ...
2564             'ylim', pointRadFact * pyRot + [-1 1] / pointZoom);
2565     elseif proj == 3
2566         set (axesPat, 'cameraViewAngle', ...
2567             2 * atan (float / (cameraDist * pointZoom)) / rpd);
2568     end
2569     clear pxRot pyRot pointRadFact
2570 end % zoom
2571 clear dirCosXmtxSurf dirCosYmtxSurf dirCosZmtxSurf;
2572 clear fore back gridPolar gridAzmth gridAzmthSmth;
2573 clear radFactSurf gridFact viewAz viewEl float radFact;
2574 end
2575
2576 drawnow;
2577
2578 end % loop over independent variable
2579 clear indx
2580
2581 % Print warnings, if any
2582 %
2583 if any (numAcc < numRlz)
2584     disp ('Warning: at least one realization could not be fully');
2585     disp (' analyzed; inspect the matfiles in the current directory.');
```

2586 end

```

2587
2588 clear cbarSize
2589 clear lx ly mx my nx ny;
2590 clear numLMX numLMY numLMNX numLMNY;
2591 clear tIndx rlzNum;
2592
2593 % end of program
2594
2595 % Suggestions for improvements
2596 %
2597 % Implement non-uniform excitation magnitudes:
2598 %
2599 % As needed, non-uniform illumination weights may be coded
2600 % straightforwardly.
2601 %
2602 % Implement element factor and improve integration of radiated powers:
2603 %
2604 % Currently the element factor is implicitly coded as one everywhere,
2605 % so that the elements radiate uniformly into the hemisphere. A more
2606 % realistic element factor is cos polar [1], being one at broadside
2607 % and zero at grazing. Note, however, that in integrating the data
2608 % over solid angles to calculate radiated powers, we divide the data
2609 % by cos polar. Performing this multiplication and division in
2610 % succession could yield invalid data near grazing, where cos polar is
2611 % small. Obviously, this difficulty could be avoided by maintaining
2612 % the unscaled data for use in the integration while using the scaled
2613 % data for all other processing. The calculations of the pointing
2614 % vector from the excitation phases and of the peak power should also
2615 % account for the element factor.
2616 %
2617 % More generally, one might wish to apply an arbitrary element factor.
2618 % If it is small near grazing, the difficulty described above
2619 % persists. One solution is to specify the element factor relative to
2620 % cos polar; the user ensures that all values of that ratio are
2621 % reasonable. The data used in the integration are scaled by the
2622 % ratio, while the data used elsewhere are scaled by both the ratio
2623 % and cos polar. One could also allow element factors defined over
2624 % the entire sphere, including radiation into z < 0, perhaps by
2625 % storing the back radiation pattern in a second g matrix and
2626 % modifying the analysis routines.
2627 %
2628 % Broadening our perspective, we note that these problems are
2629 % ultimately due to the integration algorithm, in that it blindly
2630 % applies a Jacobian that diverges at grazing. One consequence is
2631 % that data cells whose centers are just inside the border of visible
2632 % space contribute their entire value scaled by a large Jacobian,
2633 % whereas those whose centers are just outside contribute nothing.
2634 % More correctly, both should contribute about half of their value
2635 % scaled according to some average location of the contributing
2636 % region. Cells almost entirely outside of visible space should
2637 % contribute very little. A better algorithm would reproduce this
2638 % behavior.
2639 %
2640 % Allow pattern cuts:
2641 %
2642 % Often one is interested in a cut of the pattern along a path on the
2643 % unit hemisphere, such as cuts through the main beam along azimuth
2644 % and elevation curves or along the great circles of maximum and
2645 % minimum beam width. If only a graphical presentation is desired,
2646 % the cut could be interpolated from the pattern. If an analysis is
```

```

2647 % also desired, specialized routines would probably be required, as
2648 % the current routines expect data over two directional coordinates.
2649 %
2650 % Consider alternate calculation of beam widths and roll:
2651 %
2652 % The beam widths and roll are derived from an ellipse fitted to a
2653 % level contour of the main beam. Currently the fit is performed in
2654 % the boresight-centered stereographic projection regardless of the
2655 % pointing vector. This projection preserves the orientation and
2656 % orthogonality of the major and minor axes of the ellipse. However,
2657 % because scale in the stereographic projection increases away from
2658 % boresight, off-boresight contours are expanded toward the edge of
2659 % the projection. Although scale is uniform in all directions for an
2660 % infinitesimal region, radial scale is exaggerated relative to
2661 % azimuthal scale for a finite region. For a broad beam off
2662 % boresight, the distortion of beam width may be significant.
2663 %
2664 % An improvement might be achieved with two changes. First, center
2665 % the projection on the pointing vector, assuming that the contour
2666 % will be found to lie centered on the pointing vector as well.
2667 % Second, instead of the stereographic projection, use the azimuthal
2668 % equidistant projection, for which distances measured on a line
2669 % passing through the center of the projection are true. Regardless
2670 % of beam width, the lengths of the major and minor axes of the
2671 % projected ellipse will equal those of the ellipse on the hemisphere,
2672 % provided that the center of the ellipse is also the center of the
2673 % projection.
2674 %
2675 % In centering the projection on the pointing vector, one is free to
2676 % choose the orientation of the projection relative to the spherical
2677 % coordinate system, and a judicious choice of this angle facilitates
2678 % calculation of the beam's roll angle. Construct at boresight on the
2679 % hemisphere two tangent axes u and v; let positive u be directed
2680 % toward spherical azimuth zero and positive v toward  $\pi/2$ . Next,
2681 % construct the arc connecting boresight with the pointing vector.
2682 % Translate the u-v origin and system along this arc without rotation
2683 % in the plane locally tangent to the hemisphere, so that u, v, and
2684 % the arc maintain the same local orientation. If the ellipse is
2685 % centered on the pointing vector, the roll angle will be the angle
2686 % from the positive u axis to the major axis.
2687 %
2688 % Allow linear arrays:
2689 %
2690 % The current analysis routines cannot handle linear arrays because of
2691 % several incompatibilities. For example, the main beam of
2692 % one-dimensional arrays with isotropic element patterns is a cone
2693 % about the axis of the array, so the direction of radiation is
2694 % specified by a single number -- the angle between the axis and the
2695 % cone. However, the current analysis routines seek a two-parameter
2696 % specification of the main beam direction and will generally fail.
2697 % Likewise, the beam width is described by one number, but the current
2698 % routines seek two parameters. Furthermore, analyses that depend on
2699 % these values (such as determining the proximity of sidelobes) will
2700 % also fail. If linear arrays are of interest, the analysis routines
2701 % must be expanded. One might also add graphics routines tailored to
2702 % one-dimensional arrays.
2703 %
2704 % Note that a non-isotropic element pattern will generally produce a
2705 % variation in the direction orthogonal to the main beam contour,
2706 % allowing the analysis routines to proceed. Results thereby obtained
2707 % should be interpreted accordingly. (Using a non-isotropic element
2708 % pattern will not benefit the routine that locates the pointing
2709 % vector from the excitation phases. One might ignore its results
2710 % when the final pointing vector is calculated, using only the
2711 % pointing vector obtained from the Fourier transform.)
2712 %
2713 % [1] R. Tang and R. W. Burns, "Phased Arrays," in Antenna
2714 % Engineering Handbook, 3rd ed., R. C. Johnson, Ed. New York, NY:
2715 % McGraw-Hill, 1993, Ch. 20, Sec. 3.

```

## REFERENCES

1. R. J. Mailloux, "Array grating lobes due to periodic phase, amplitude, and time delay quantization," *IEEE Trans. Antennas and Propagation*, vol. 32, pp. 1364–1368, Dec. 1984.
2. A. P. Goutzoulis and D. K. Davies, "Switched fiber optic delay architectures," in *Photonic Aspects of Modern Radar*, H. Zmuda and E. N. Toughlian, Eds. Boston, MA: Artech House, 1994, pp. 351–380.
3. A. K. Agrawal and E. L. Holzman, "Beamformer architectures for active phased-array radar antennas," *IEEE Trans. Antennas and Propagation*, vol. 47, pp. 432–442, Mar. 1999.
4. R. J. Mailloux, *Phased Array Antenna Handbook*, ch. 7. Norwood, MA: Artech House, 1994.
5. R. C. Hansen, *Phased Array Antennas*, Sec. 12.4. New York: John Wiley & Sons, 1998.
6. B. D. Steinberg, *Principles of Aperture and Array System Design*, ch. 13. New York: John Wiley & Sons, 1976.
7. B. P. Chrisman, "Planar array antenna design analysis," in *Proc. Tactical Communications Conf.*, 1990, vol. 1, pp. 705–731.
8. P. J. Wright, "Simulation of phased array antennas," in *Tenth International Conf. on Antennas and Propagation*, 1997, vol. 1, pp. 498–501.
9. A. K. Agrawal, E. L. Williamson, and J. G. Ferrante, "Design criteria for wideband active phased array antennas," in *IEEE Antennas and Propagation Society International Symposium 1997 Digest*, vol. 2, pp. 714–717.
10. J. J. Lee et al., "Photonic wideband array antennas," *IEEE Trans. Antennas and Propagation*, vol. 43, pp. 966–982, Sept. 1995.
11. The MathWorks, Inc., 3 Apple Hill Dr., Natick, MA 01760-2098.
12. J. P. Snyder, *Map Projections: A Working Manual*, US Geological Survey Professional Paper 1395. Washington, DC: United States Government Printing Office, 1987.
13. D. H. von Seggern, *CRC Standard Curves and Surfaces*. Boca Raton, FL: CRC, 1993.
14. R. S. Elliott, "Beamwidth and directivity of large scanning arrays," *Microwave J.*, vol. 7, pp. 74–82, Jan. 1964.
15. R. S. Elliott, "The Theory of Antenna Arrays," in *Microwave Scanning Antennas*, vol. 2, R. C. Hansen, Ed. New York: Academic, 1966, pp. 1–69.